CONFIDENTIAL

Copy 235
RM L55A12

NACA RM L55A12

7699

TECH LIBRARY KAFB, NM
0144194

NACA

RESEARCH MEMORANDUM

EXPERIMENTAL STATIC AERODYNAMIC FORCES AND MOMENTS AT LOW SPEED ON A CANARD MISSILE DURING SIMULATED LAUNCHING FROM THE MIDSEMISPAN AND WING-TIP LOCATIONS OF A 45° SWEPTBACK WING-FUSELAGE COMBINATION

By William J. Alford, Jr.

Langley Aeronautical Laboratory
Langley Field, Va.

CLASSIFIED DOCUMENT

This material contains information affecting the National Defense of the United States within the meaning of the espionage laws, Title 18, U.S.C., Secs. 793 and 794, the transmission or revelation of which in any manner to an unauthorized person is prohibited by law.

NATIONAL ADVISORY COMMITTEE
FOR AERONAUTICS

WASHINGTON
April 6, 1955

CONFIDENTIAL

TECH LIBRARY KAFB, NM
0144194

NATIONAL ADVISORY COMMITTEE FOR AERONAUTICS

RESEARCH MEMORANDUM

EXPERIMENTAL STATIC AERODYNAMIC FORCES AND MOMENTS AT LOW SPEED ON A CANARD MISSILE DURING SIMULATED LAUNCHING FROM THE MIDSEMISPAN AND WING-TIP LOCATIONS OF A 45° SWEPTBACK WING-FUSELAGE COMBINATION

By William J. Alford, Jr.

SUMMARY

An investigation was made at low speed to determine the static aerodynamic forces and moments on a canard missile model during simulated launching from the midsemispan and wing-tip locations of a wing-fuselage combination having a 45° sweptback wing. The results indicated that, when the missile was mounted under the wing at the midsemispan location, changes in chordwise position generally produced large changes in missile forces and moments, with these changes becoming larger as the angle of attack was increased. Free-air conditions were approached when the missile was moved forward to a location about 1.0 to 1.5 wing-chords distance ahead of the leading edge of the wing-fuselage combination. The influence of the wing fuselage was reduced as the missile was moved downward, and the degree of reduction depended on the longitudinal location of the missile. The effects of three degrees of incidence of sideslip on the static aerodynamic forces and moments of the missile relative to the wing-fuselage combination generally were small in comparison with the effects of either longitudinal displacement of the missile or angle of attack of the wing-fuselage combination. When the missile was mounted at the wing tip, the changes in missile forces and moments with changes in chordwise position were generally smaller than the changes noted with the missile mounted under the wing. However, because of the presence of the wing-tip vortex, the missile rolling moments were considerably larger for the tip location.

INTRODUCTION

The National Advisory Committee for Aeronautics is conducting investigations to determine the nature and origin of the mutual interference effects experienced by various wing-fuselage models and various types of external stores. Previous investigations (refs. 1 to 3) have shown the

existence of these generally objectionable interference effects, and reference 4 has shown that, at low speeds, they are primarily due to the nonuniform flow field generated in the vicinity of the model. The severity of these induced effects on the force and moment characteristics of a conventional missile model (with the tail located aft of the wing) has been reported in reference 5.

This paper presents the low-speed static aerodynamic forces and moments on a canard missile model during simulated launch from the mid-semispan and wing-tip locations of a wing-fuselage combination having a 45° sweptback wing. The effects of changes in missile incidence and sideslip angle relative to the wing-fuselage combination are also shown. In order to expedite publication of these data only a brief analysis is presented.

SYMBOLS

N	missile normal force, lb
m	missile pitching moment, ft-lb
A	missile axial force, lb
Y	missile side force, lb
n	missile yawing moment, ft-lb
l	missile rolling moment, ft-lb
C_N	missile normal-force coefficient, $N/qS_{(m)}$
C_m	missile pitching-moment coefficient, $\frac{m}{qS_{(m)}d_{(m)}}$
C_A	missile axial-force coefficient, $\frac{A}{qS_{(m)}}$
C_Y	missile side-force coefficient, $\frac{Y}{qS_{(m)}}$
C_n	missile yawing-moment coefficient, $\frac{n}{qS_{(m)}d_{(m)}}$
C_l	missile rolling-moment coefficient, $\frac{l}{qS_{(w)}b_{(m)}}$

C_L	lift coefficient of wing-fuselage combination, $\frac{\text{Lift}}{qS}$
q	free-stream dynamic pressure, lb/sq ft
V_o	free-stream velocity, ft/sec
$S_{(m)}$	missile body maximum cross-sectional area, 0.0131 sq ft
S_w	exposed area of two missile wing panels, 0.0357 sq ft
S	wing area of wing-fuselage combination, 6.25 sq ft
$b_{(m)}$	span of missile wing, 0.384 ft
b	span of wing-fuselage combination, 5 ft
$d_{(m)}$	maximum diameter of missile body, 1.55 in.
c	local wing chord of wing-fuselage combination, ft
x	chordwise distance from leading edge of local wing chord to missile center of gravity, positive aft (fig. 1), ft
y	spanwise distance from fuselage center line to missile center line (fig. 1), ft
z	vertical distance from wing-chord plane, positive up (fig. 1), ft
L	fuselage length, 7.61 ft
α	angle of attack of wing-fuselage combination, deg
$\alpha_{(m)}$	angle of attack of missile center line (fig. 2), deg
$i_{(m)}$	angle of incidence between missile center line and wing-chord line, deg
$\beta_{(m)}$	angle of sideslip between missile center line and fuselage center line, deg

Subscripts:

(m)	missile body
(w)	missile wings

MODELS AND APPARATUS

The wing of the wing-fuselage combination used as the test vehicle had a 45° sweptback quarter-chord line, an aspect ratio of 4.0, a taper ratio of 0.3, and employed NACA 65A006 airfoil sections parallel to the free-stream direction. The fuselage consisted of an ogival nose section, a cylindrical center section, and a truncated tail cone. A two-view drawing of the wing-fuselage combination as part of the test setup is shown in figure 1 and the fuselage ordinates are presented in table I.

The canard missile model used in this investigation employed a cruciform arrangement of its wings and canard fins and is shown in figure 1 as part of the test setup. Details of the missile model are shown in figure 3. Figure 4 is a photograph of the test setup with the missile model installed at the midsemispan location. The missile was internally instrumented with a six-component strain-gage balance and was supported from the rear of the wing-fuselage combination by a sting that was adjustable in the longitudinal, lateral, and vertical directions (fig. 1). The missile center line was located at the one-half semispan station at several vertical heights and at the 1.04-semispan station with its center line in the plane of the wing chord and parallel to the wing-tip chord. A series of chordwise positions was investigated for both spanwise locations. The effects of missile center-line incidence angle and sideslip angle on the static aerodynamic forces and moments were investigated with the missile at the midsemispan location for several chordwise positions.

TESTS

The tests were made in the Langley 300 MPH 7- by 10-foot tunnel at a velocity of 125 mph, which corresponds to a dynamic pressure of 40 pounds per square foot and a Reynolds number of 1.1×10^6 per foot of a typical dimension. Measurements were made of the static aerodynamic forces and moments on the canard missile during simulated launchings from the midsemispan and wing-tip locations of a wing-fuselage combination having a 45° sweptback wing. The investigation included the effects of changes in missile incidence and sideslip angle at the midsemispan location, relative to the wing-fuselage combination. The angle-of-attack range extended from -8° to 20°.

The missile was tested under the left wing and at the left wing tip of the test vehicle, which was inverted so as to avoid support-strut interference (fig. 4). The directions of positive forces and moments are as shown in figure 2.

CORRECTIONS AND ACCURACY

Blockage corrections were applied to the dynamic pressure by use of the method of reference 6, and jet-boundary corrections calculated by the method of reference 7 have been applied to the angle of attack. In addition, an angle-of-attack correction of 0.2° was applied to account for the tunnel free-stream misalinement angle.

A study of the missile model strain-gage-balance calibrations and the general repeatability of the test data indicated that the accuracy levels of the various force and moment coefficients are approximately as follows:

Component	Accuracy
C_N	±0.25
C_m	±0.25
C_A	±0.05
C_Y	±0.25
C_n	±0.25
C_l	±0.005

RESULTS AND DISCUSSION

The aerodynamic characteristics of the isolated missile at low speed, as determined from breakdown tests in the free stream, are presented in figure 5. The basic data of the missile model when it is in the proximity of the wing-fuselage combination are presented as a function of angle of attack in figures 6 to 9, and are presented as a function of chordwise position in figures 10 and 11. The lift characteristics of the isolated wing-fuselage combination are presented for orientation in figure 12.

Figures 6 to 10 indicate that changes in chordwise position of the missile at the midsemispan location produce large changes in the forces and moments of the missile in both the longitudinal and lateral planes. As would be expected, the changes in the static aerodynamic forces and moments of the missile induced by the wing-fuselage combination, diminish as the missile is moved ahead of the wing. When the missile center of gravity reaches a distance of 1.0 to 1.5 wing chords ahead of the leading edge of the wing-fuselage combination, the missile forces and moments approach those of the isolated missile (see figs. 5, 6, and 10).

The effects of changes in the vertical position of the missile are also shown in figures 6 and 10. As the missile is moved away from the wing-chord plane, the changes induced by the presence of the wing-fuselage combination are seen to be generally reduced, and the degree of reduction is a function of the missile longitudinal location.

As the angle of attack is increased, the induced effects also are increased. This increase can be explained (ref. 4) by the increase in wing circulation strength which results in strengthened and expanded downwash- and sidewash-angularity fields in conjunction with a nonuniform dynamic-pressure field.

The effects of increasing the missile incidence angle (fig. 7) or the missile sideslip angle (fig. 8) to 3°, relative to the wing-fuselage combination, was small in comparison with the effects of changes in either the longitudinal displacement of the missile or the angle of attack of the wing-fuselage combination.

When the canard missile is located at the one-half semispan location, the trends of the static aerodynamic forces and moments of the present investigation agree qualitatively with the forces and moments of the conventional missile (with the tail located behind the wing) reported in reference 5.

When the missile model was mounted at the wing-tip location of the wing-fuselage combination (figs. 9 and 11), changes in the missile forces and moments were less severe than those of the missile at the midsemispan location, with the exception of the rolling moment which was greatly increased due to the effect of the wing-tip vortex (figs. 6, 9, 10, and 11). As the missile center of gravity was moved ahead of the wing leading edge, the missile forces and moments generally diminished and approached the isolated missile values between 1.0 and 1.5 wing chords ahead of the wing leading edge.

CONCLUSIONS

The results of an investigation at low speed of the static aerodynamic forces and moments on a canard missile model during simulated launching from the midsemispan and wing-tip locations of a wing-fuselage combination having a 45° sweptback wing, indicate the following conclusions:

1. When the missile was mounted under the wing at the midsemispan location, changes in chordwise position generally produced large changes in missile forces and moments, and these changes became larger as the angle of attack was increased. Free-air conditions were approached when

the missile was moved forward to a location about 1.0 to 1.5 wing-chord distance ahead of the leading edge of the wing-fuselage combination. The influence of the wing fuselage was reduced as the missile was moved downward, and the degree of reduction depended on the longitudinal location of the missile.

2. The effects of three degrees of incidence or sideslip on the static aerodynamic forces and moments of the missile relative to the wing-fuselage combination generally were small in comparison with the effects of either longitudinal displacement of the missile or angle of attack of the wing-fuselage combination.

3. When the missile was mounted at the wing tip, the changes in missile forces and moments with changes in chordwise position generally were smaller than the changes noted with the missile mounted under the wing. However, because of the presence of the wing-tip vortex, the missile rolling moments were considerably larger for the tip location.

Langley Aeronautical Laboratory,
National Advisory Committee for Aeronautics,
Langley Field, Va., January 4, 1955.

REFERENCES

1. Alford, William J., Jr., and Silvers, H. Norman: Investigation at High Subsonic Speeds of Finned and Unfinned Bodies Mounted at Various Locations From the Wings of Unswept- and Swept-Wing-Fuselage Models, Including Measurements of Body Loads. NACA RM L54B18, 1954.

2. Silvers, H. Norman, and King, Thomas J., Jr.: Investigation at High Subsonic Speed of Bodies Mounted From the Wing of an Unswept-Wing-Fuselage Model, Including Measurements of Body Loads. NACA RM L52J08, 1952.

3. Silvers, H. Norman, and Alford, William J., Jr.: Investigation at High Subsonic Speeds of the Effect of Adding Various Combinations of Missiles on the Aerodynamic Characteristics of Sweptback and Unswept Wings Combined With a Fuselage. NACA RM L54D20, 1954.

4. Alford, William J., Jr., Silvers, H. Norman, and King, Thomas J., Jr.: Preliminary Low-Speed Wind-Tunnel Investigation of Some Aspects of the Aerodynamic Problems Associated With Missiles Carried Externally in Positions Near Airplane Wings. NACA RM L54J20, 1954.

5. Alford, William J., Jr., Silvers, H. Norman, and King, Thomas J., Jr.: Experimental Aerodynamic Forces and Moments at Low Speed of a Missile Model During Simulated Launching from the Midsemispan Location of a 45° Sweptback Wing-Fuselage Combination. NACA RM L54K11a, 1955.

6. Herriot, John G.: Blockage Corrections for Three-Dimensional-Flow Closed-Throat Wind Tunnels, With Consideration of the Effect of Compressibility. NACA Rep. 955, 1950. (Supersedes NACA RM A7B28.)

7. Gillis, Clarence L., Polhamus, Edward C., and Gray, Joseph L., Jr.: Charts for Determining Jet-Boundary Corrections for Complete Models in 7- by 10-Foot Closed Rectangular Wind Tunnels. NACA WR L-123, 1945. (Formerly NACA ARR L5G31.)

TABLE I.- FUSELAGE ORDINATES

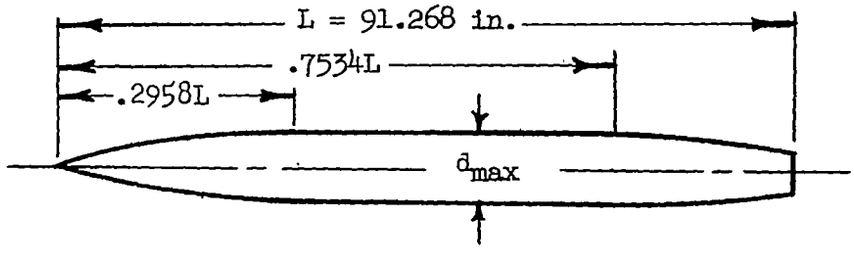

Ordinates, percent length	
Station	Radius
0	0
3.28	.91
6.57	1.71
9.86	2.41
13.15	3.00
16.43	3.50
19.72	3.90
23.01	4.21
26.29	4.43
29.58	4.57
75.34	4.57
76.69	4.54
79.98	4.38
83.26	4.18
86.55	3.95
89.84	3.72
93.13	3.49
96.41	3.26
100.00	3.02

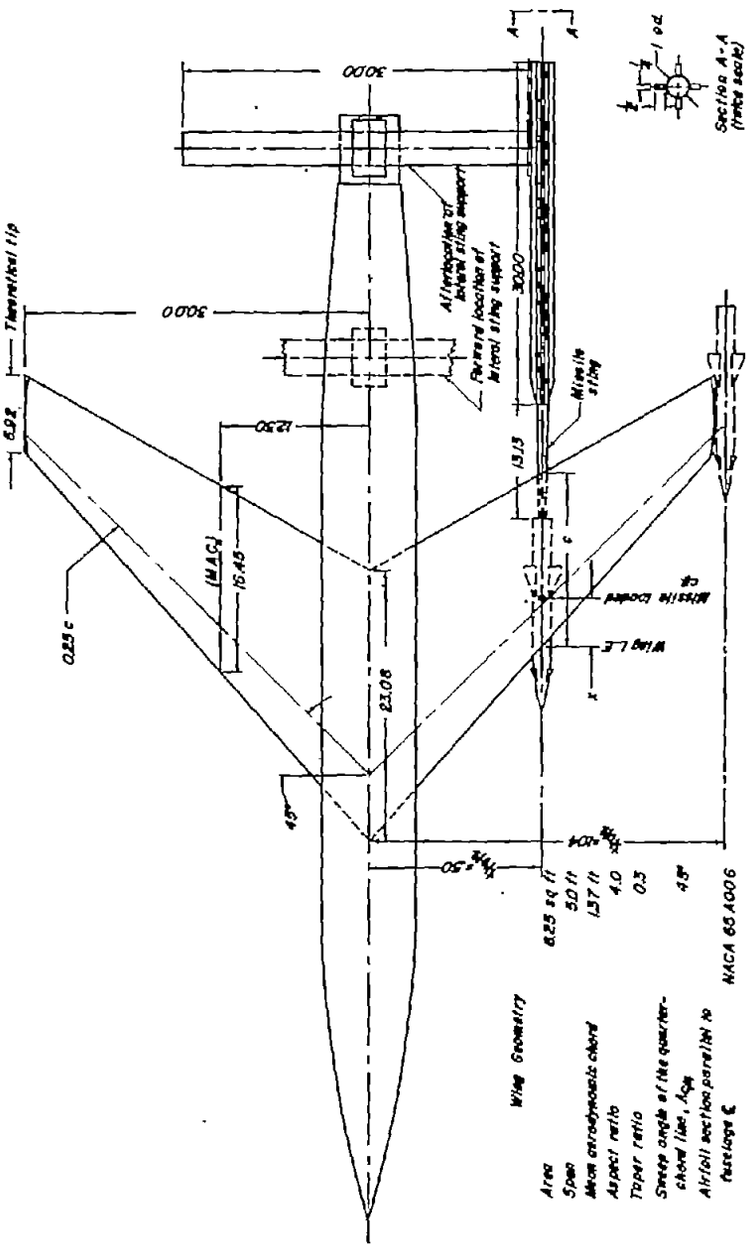

Figure 1.- Test setup showing missile in test locations. All dimensions in inches.

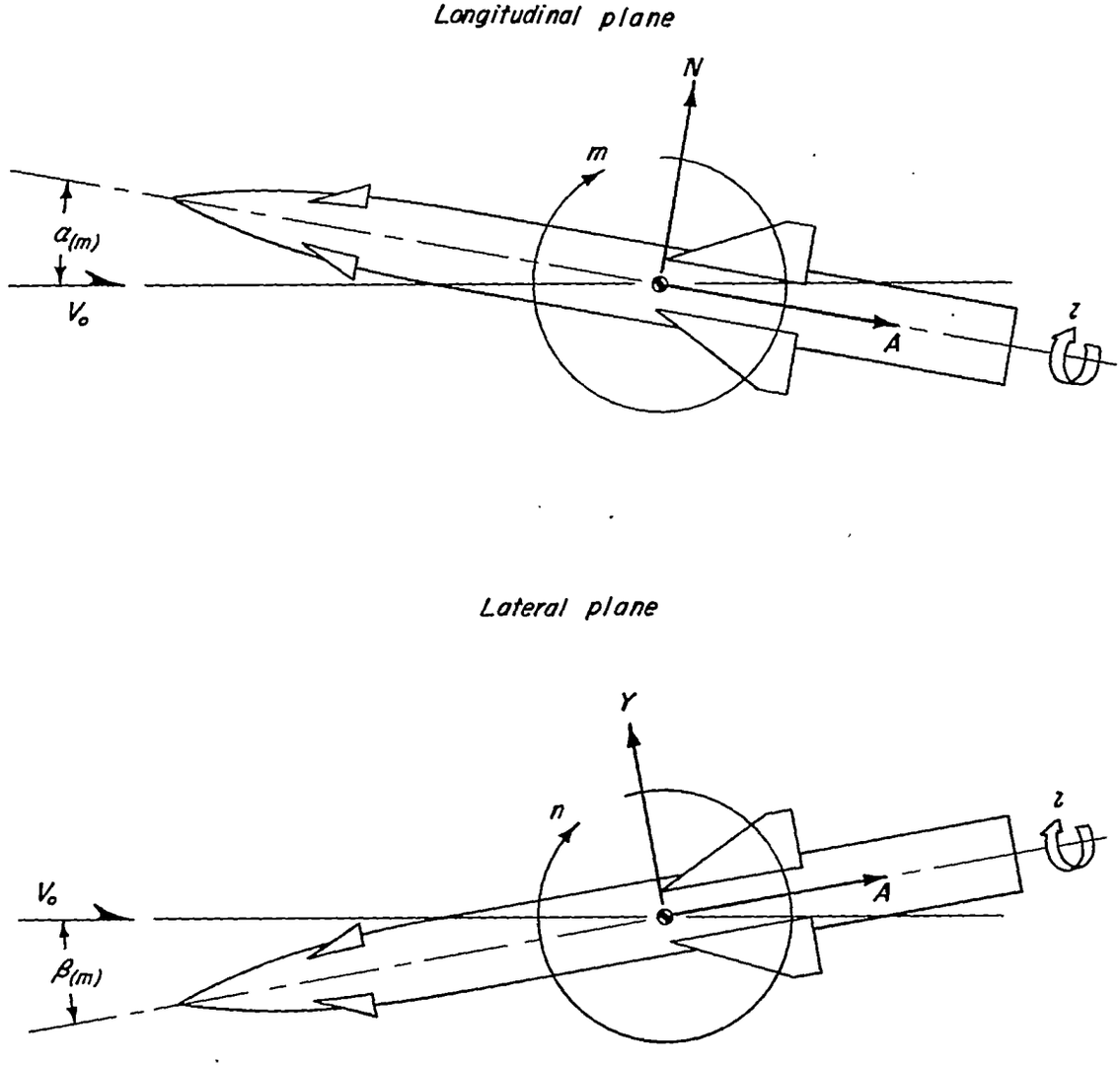

Figure 2.- Positive direction of forces and moments as measured on missile model.

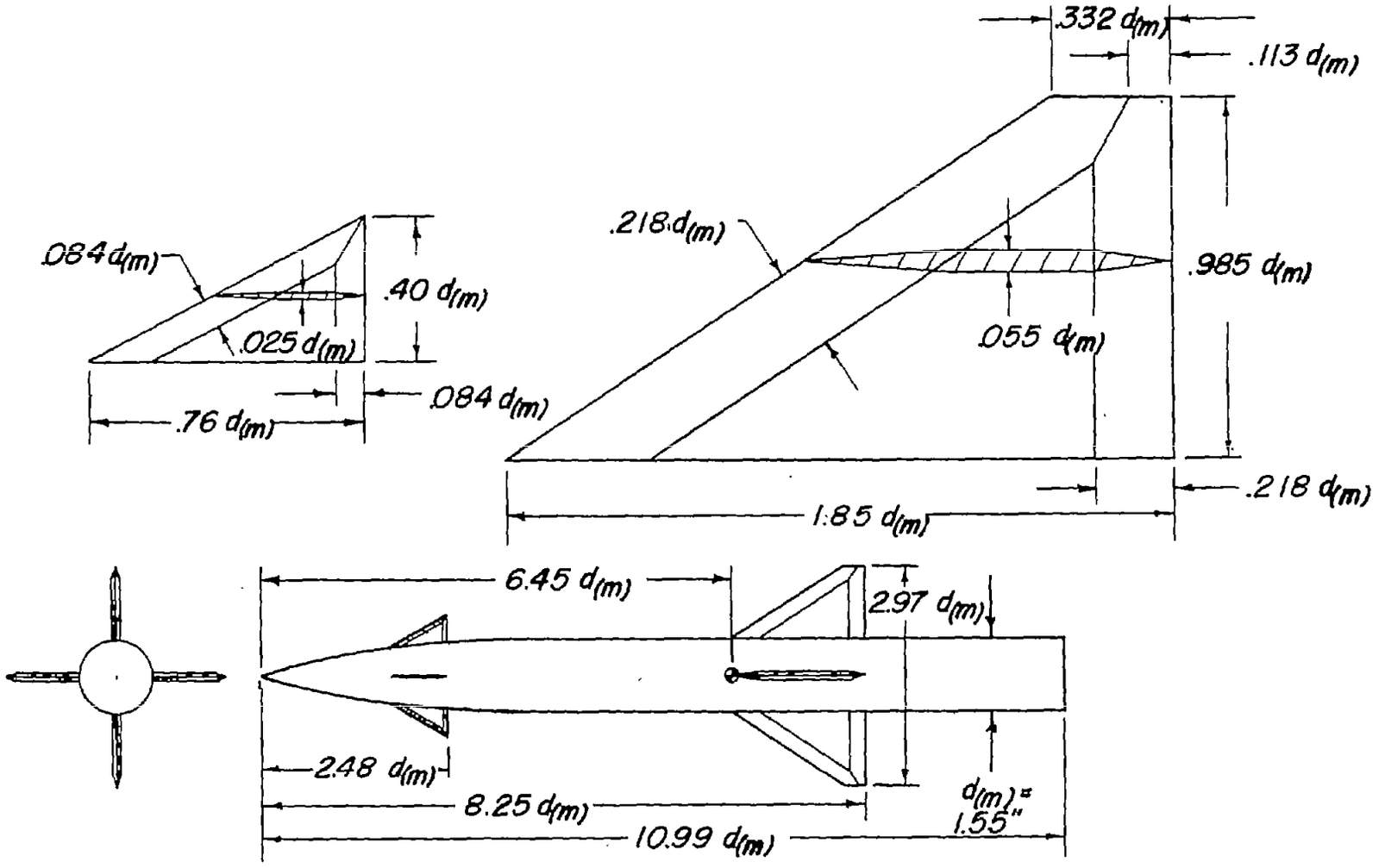

Figure 3.- Drawing of missile model showing general proportions.

L-85687

Figure 4.- Photograph of wing-fuselage combination with missile model installed.

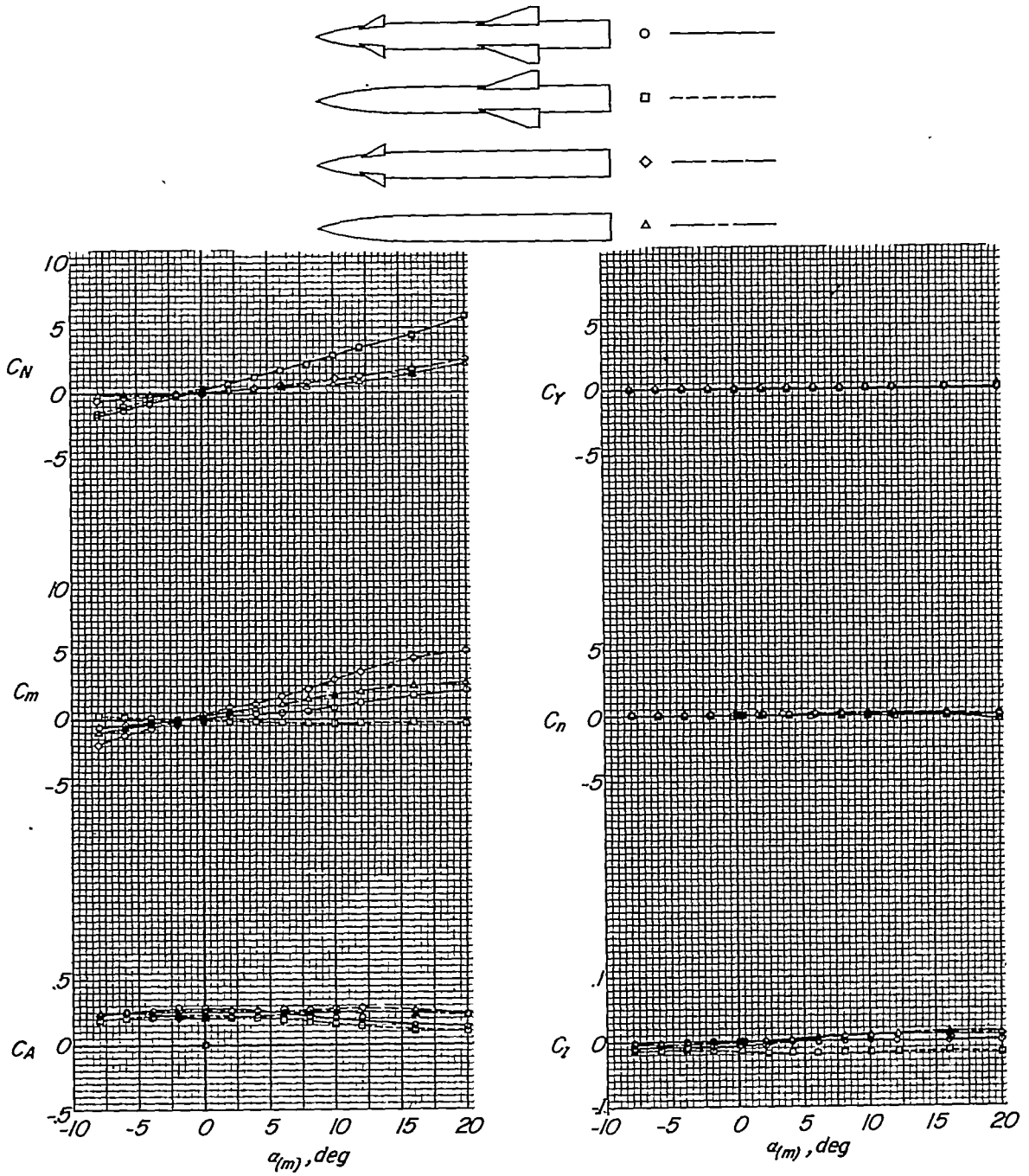

Figure 5.- Aerodynamic characteristics of isolated missile at low speed and missile component characteristics.

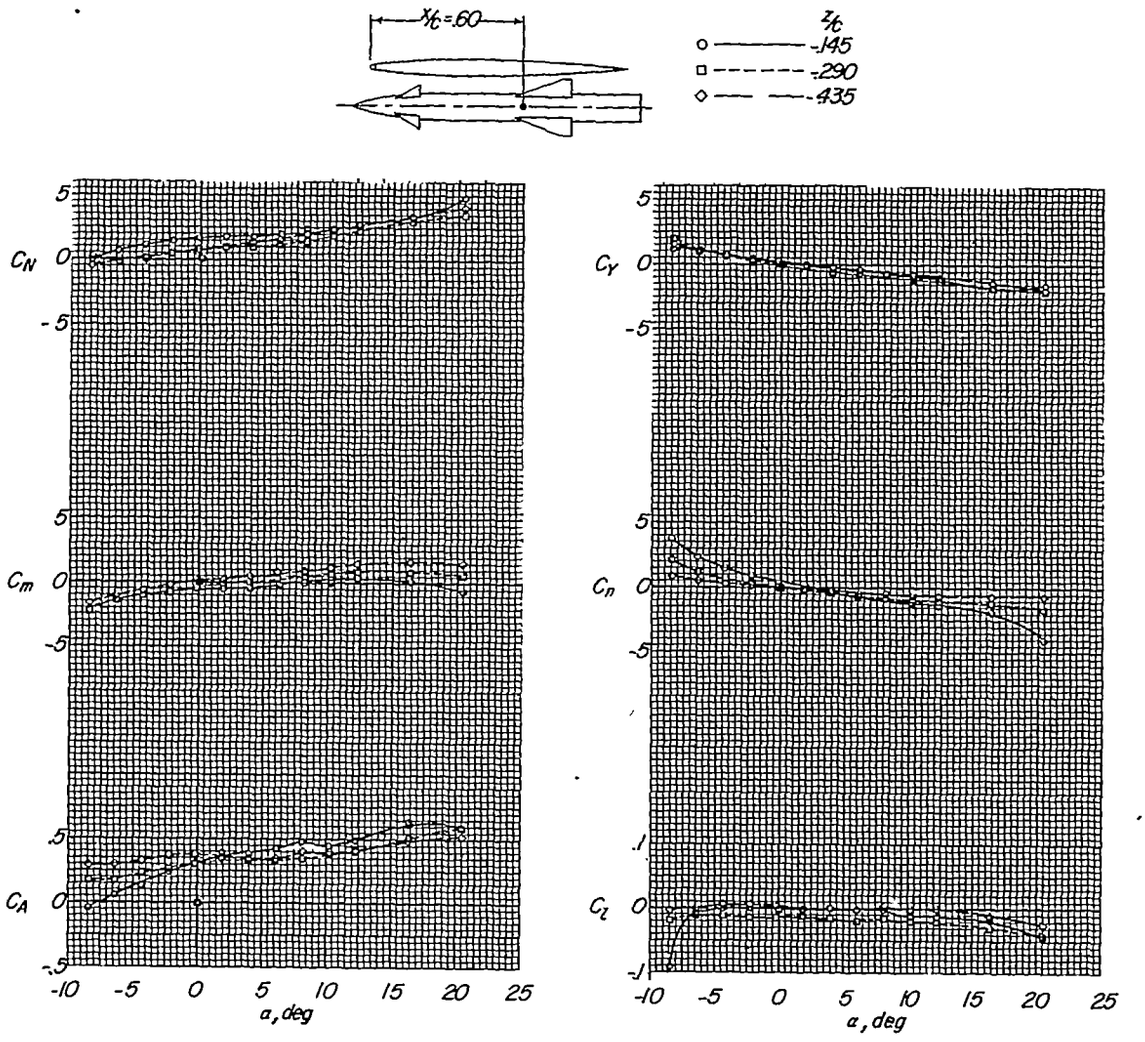

(a) x/c = 0.60.

Figure 6.- Missile aerodynamic characteristics at one-half semispan station as affected by wing-fuselage combination.

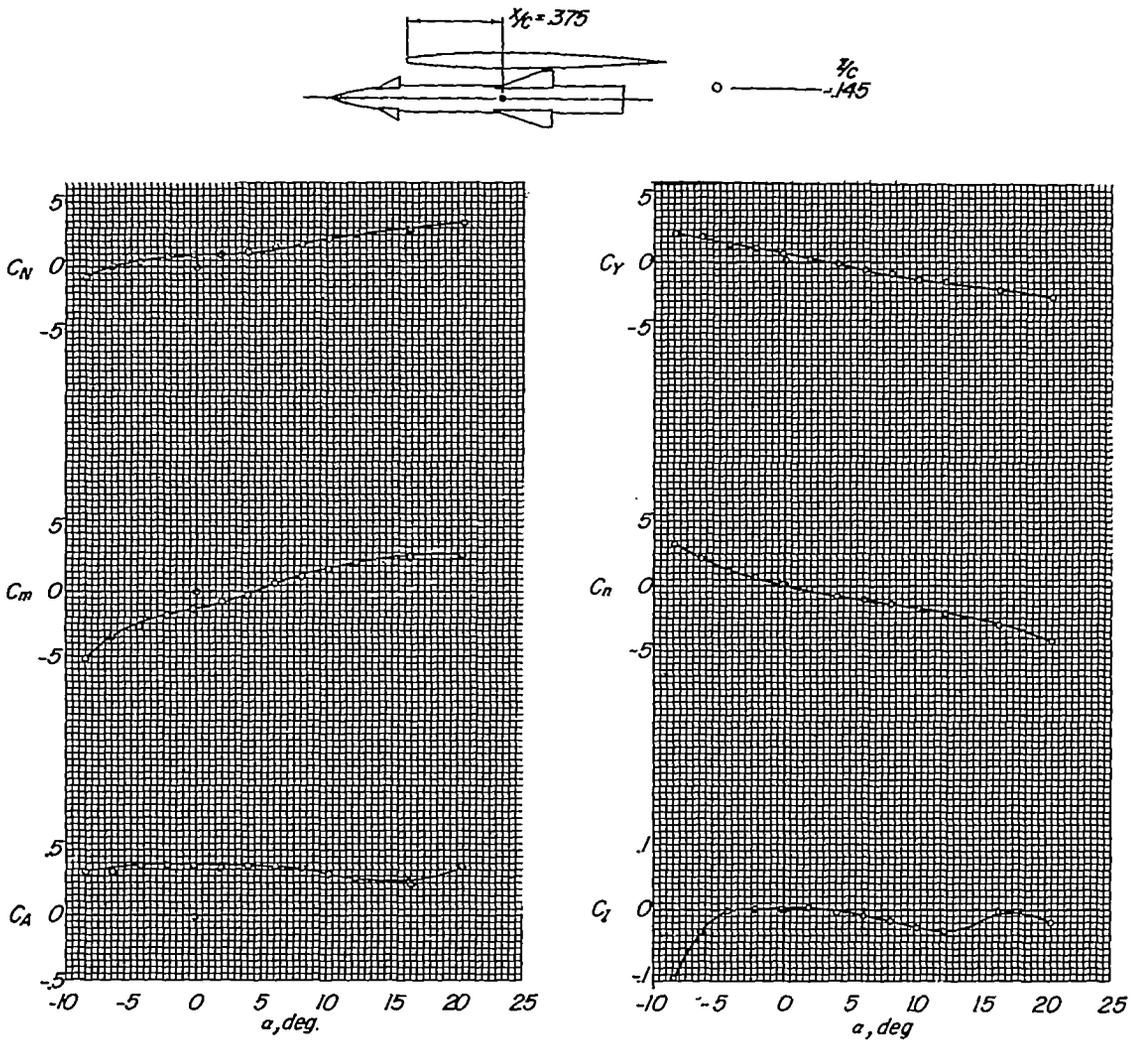

(b) x/c = 0.375.

Figure 6.- Continued.

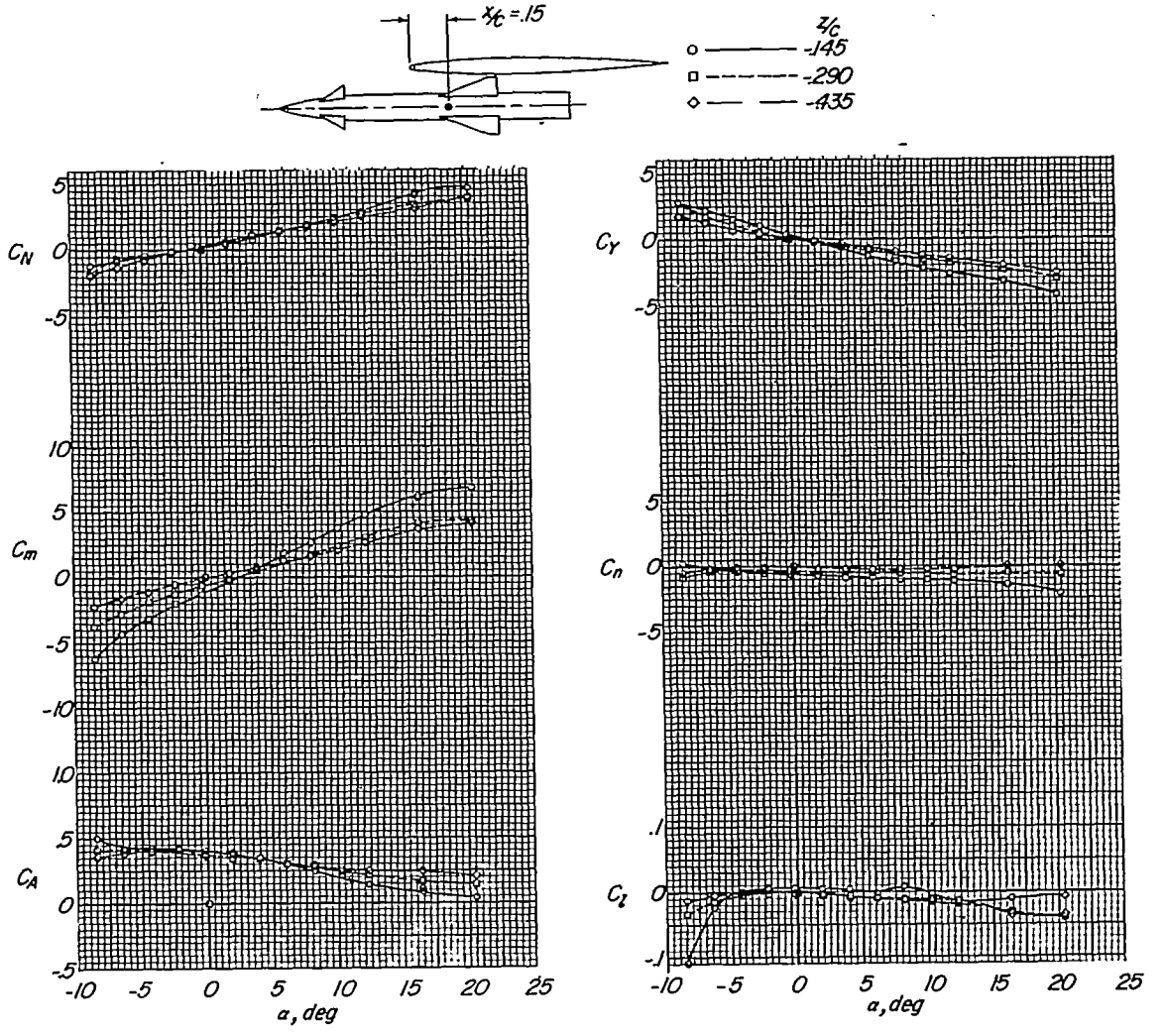

(c) x/c = 0.15.

Figure 6.- Continued.

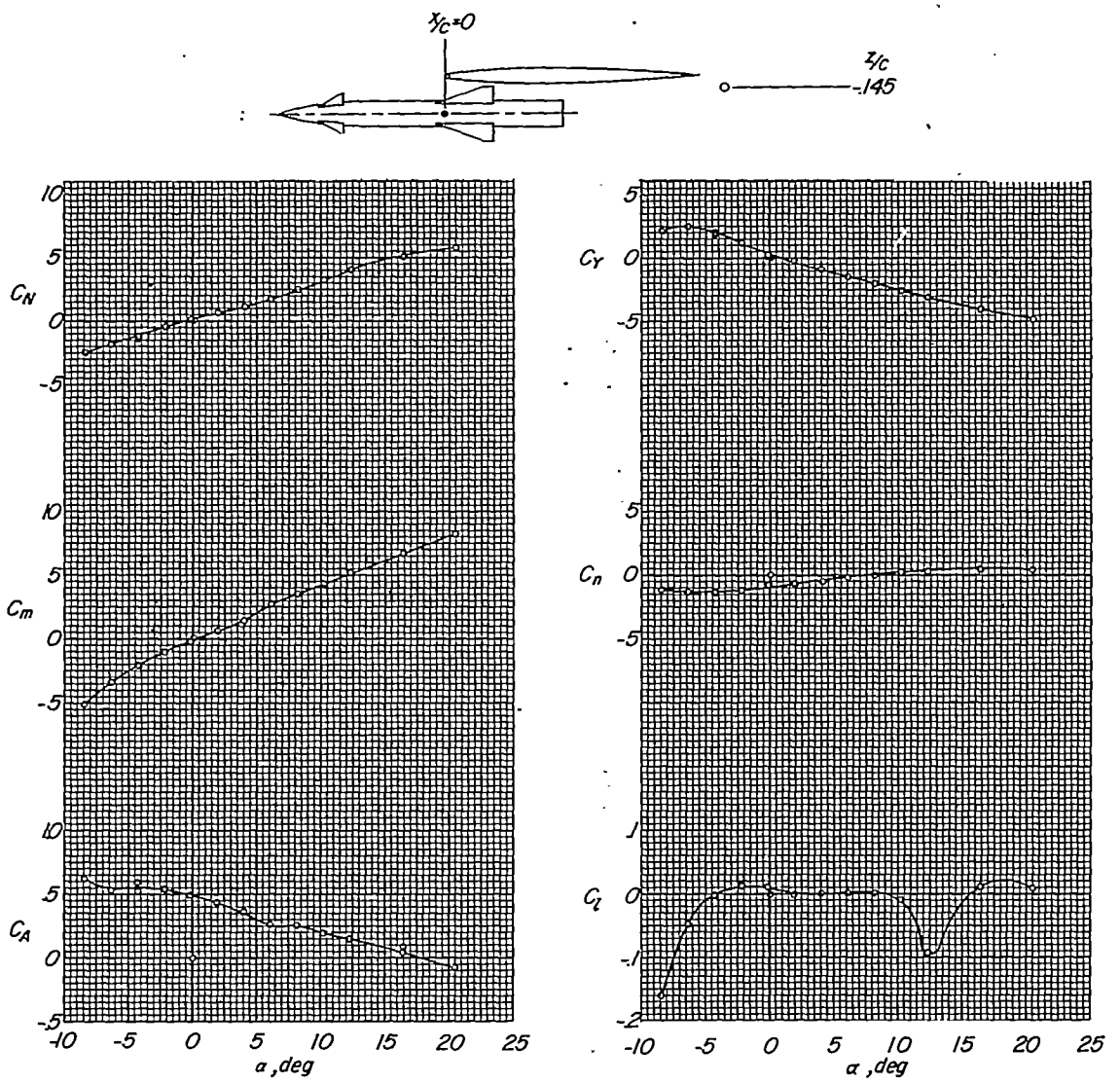

(d) x/c = 0.

Figure 6.- Continued.

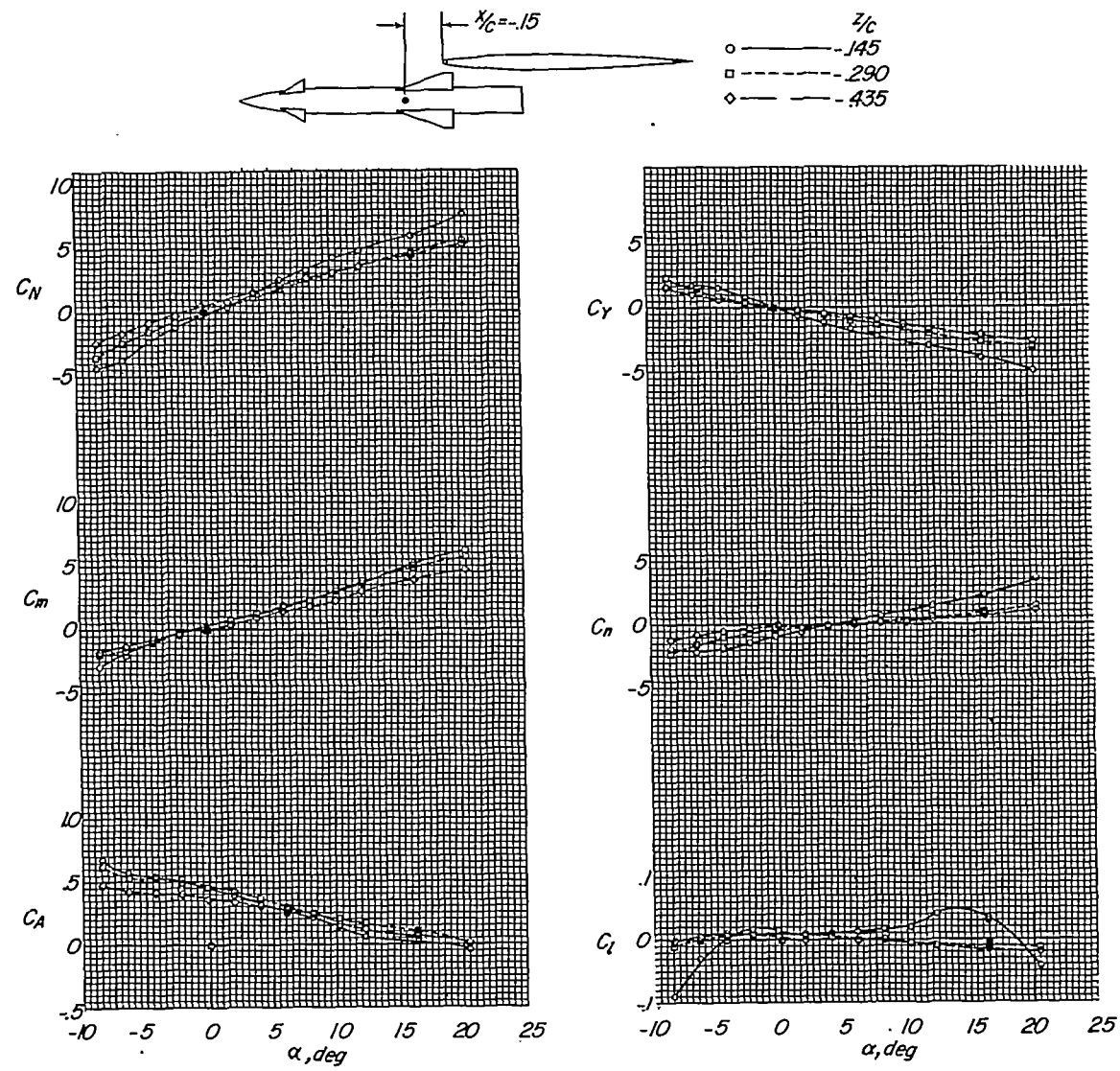

(e) x/c = -0.15.

Figure 6.- Continued.

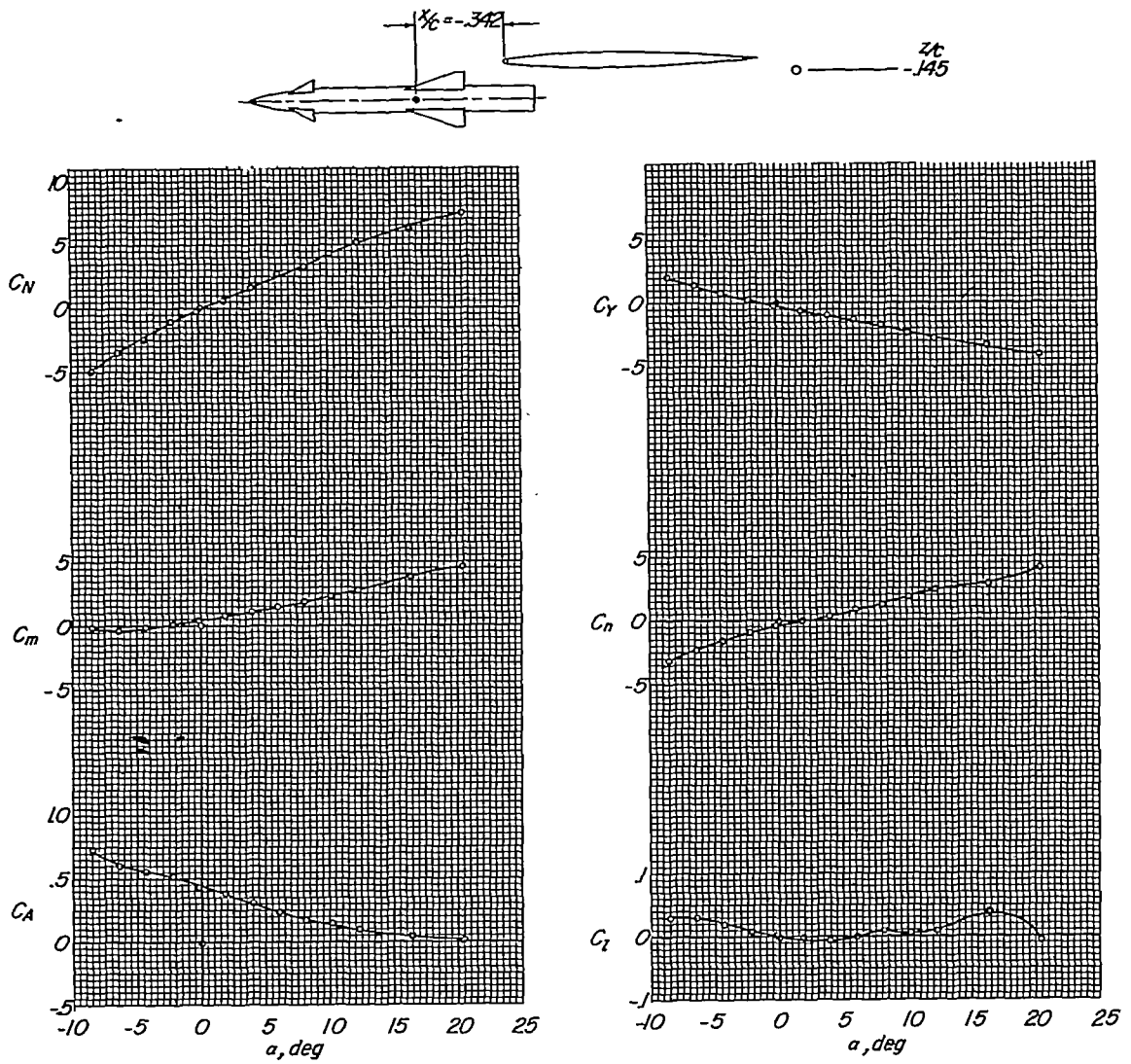

(f) x/c = -0.342.

Figure 6.- Continued.

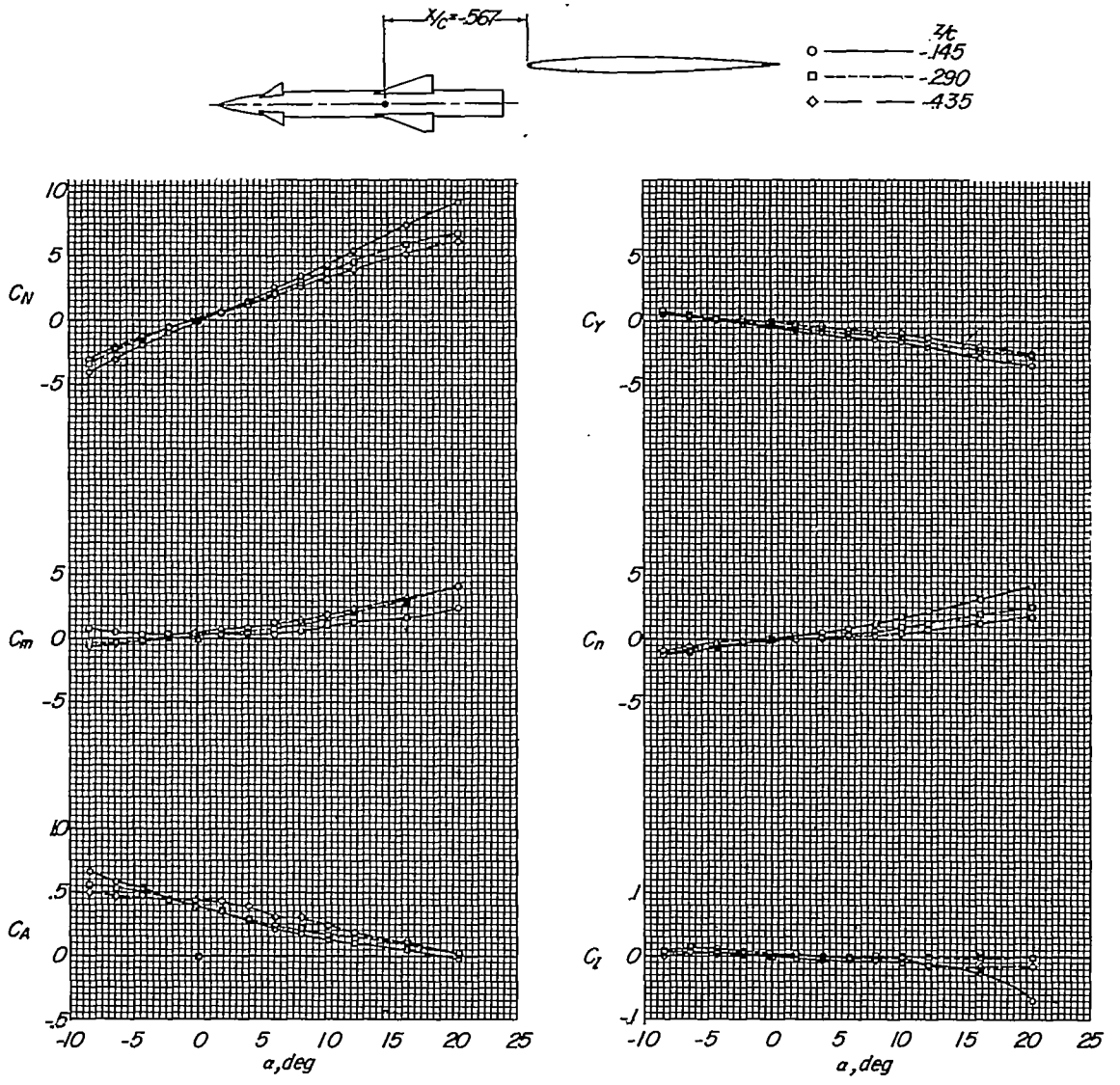

(g) x/c = -0.567.

Figure 6.- Continued.

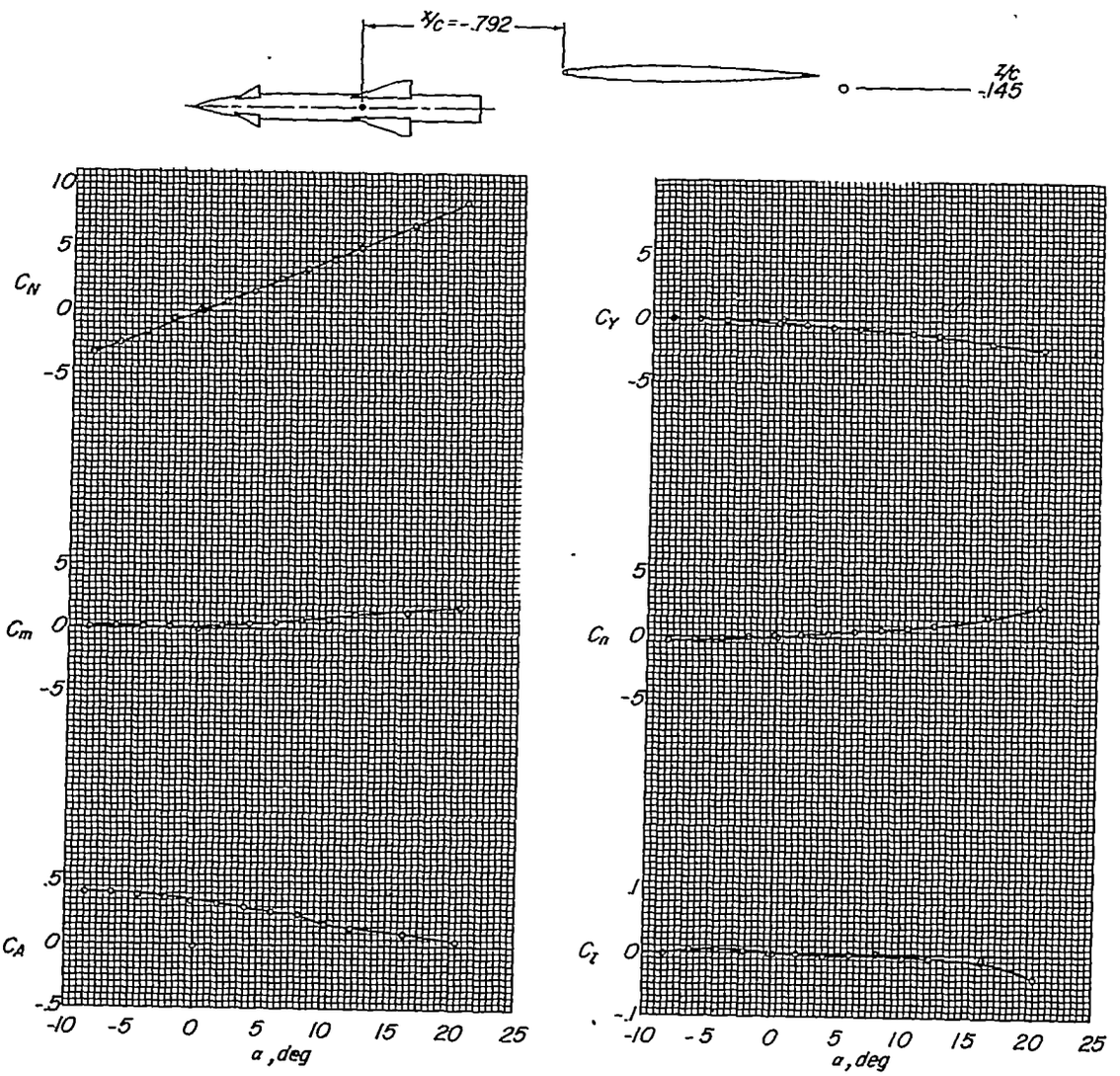

(h) x/c = -0.792.

Figure 6.- Continued.

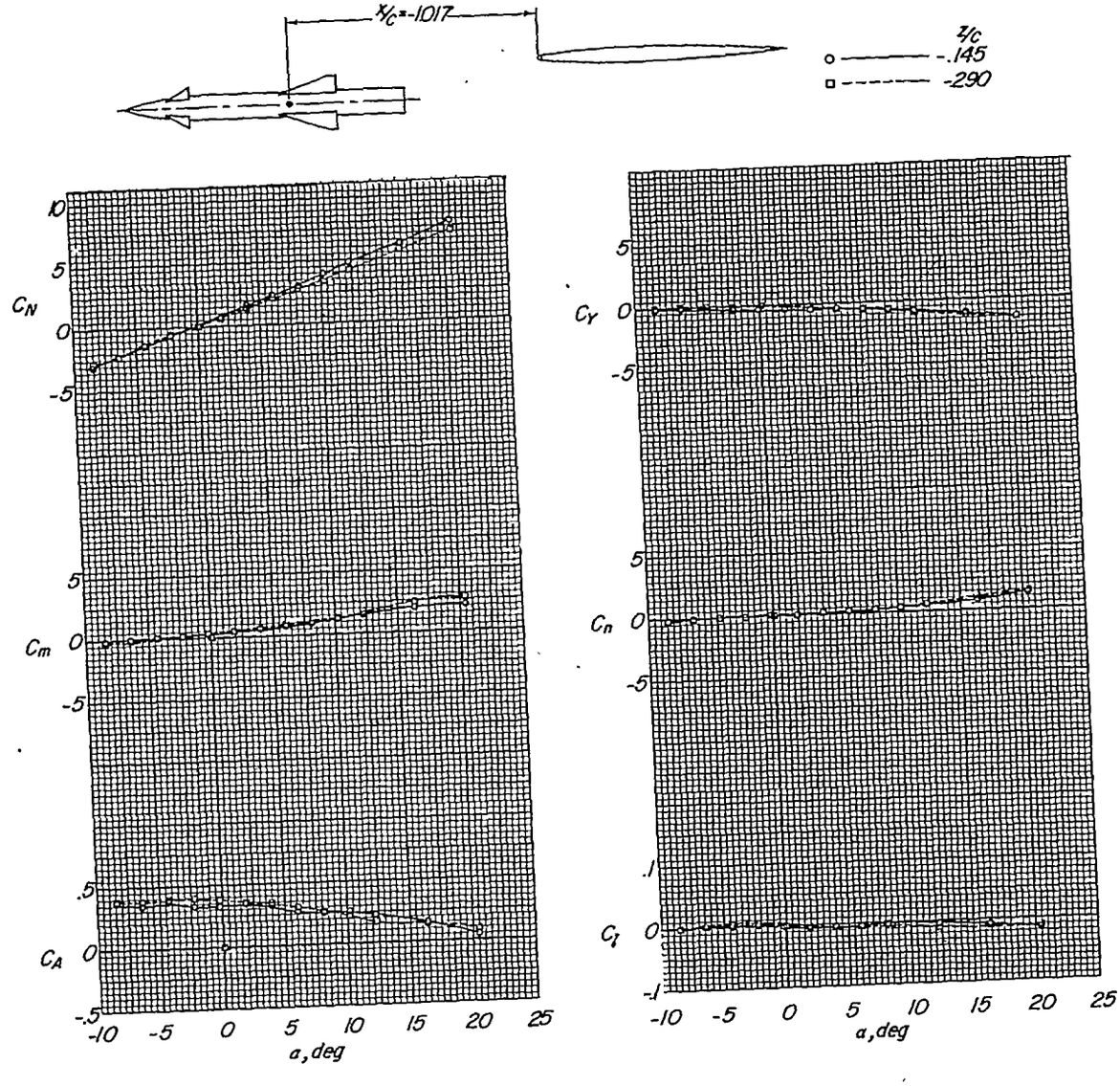

(i) x/c = -1.017.

Figure 6.- Continued.

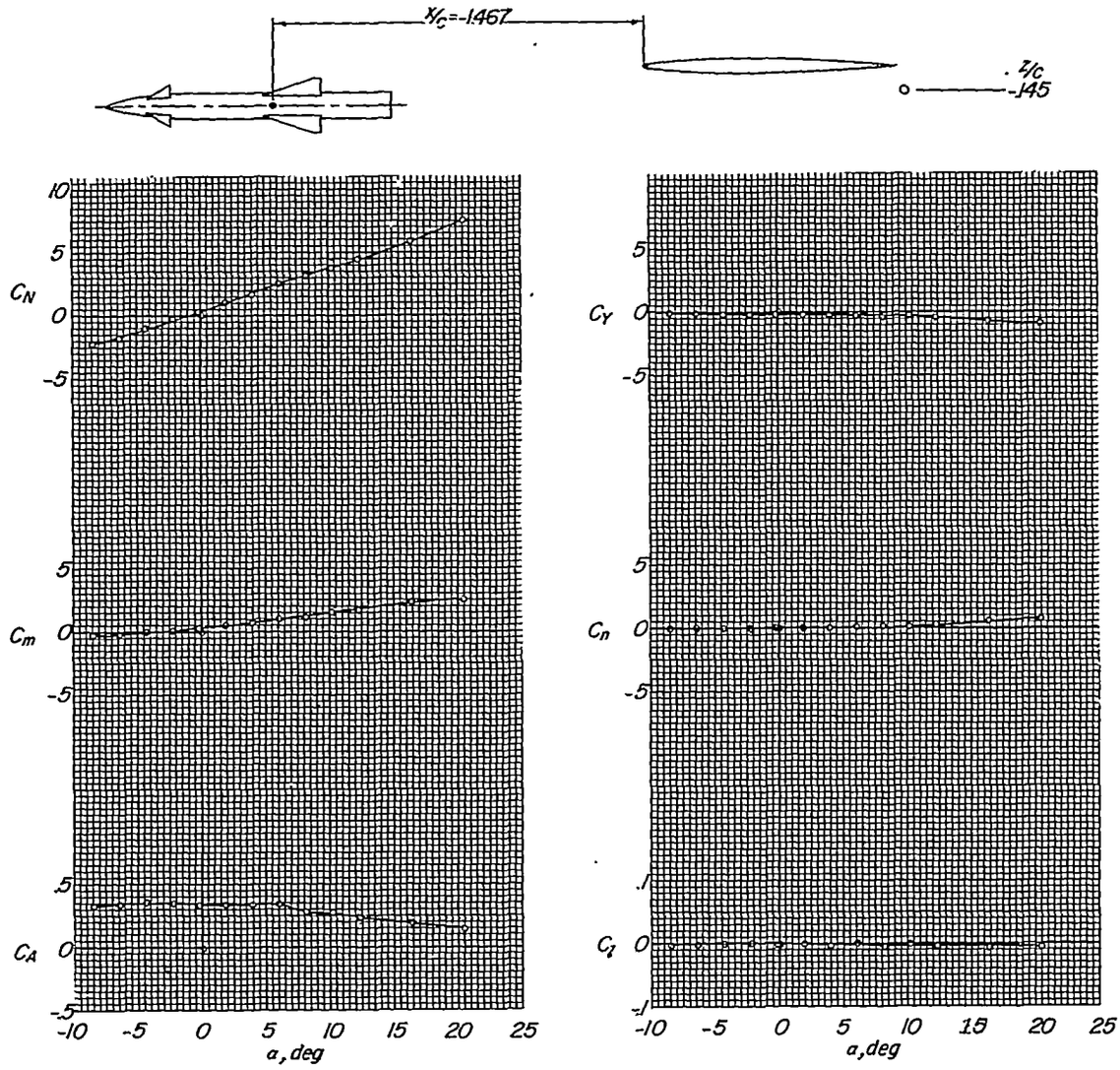

(j) x/c = -1.467.

Figure 6.- Concluded.

[redacted]

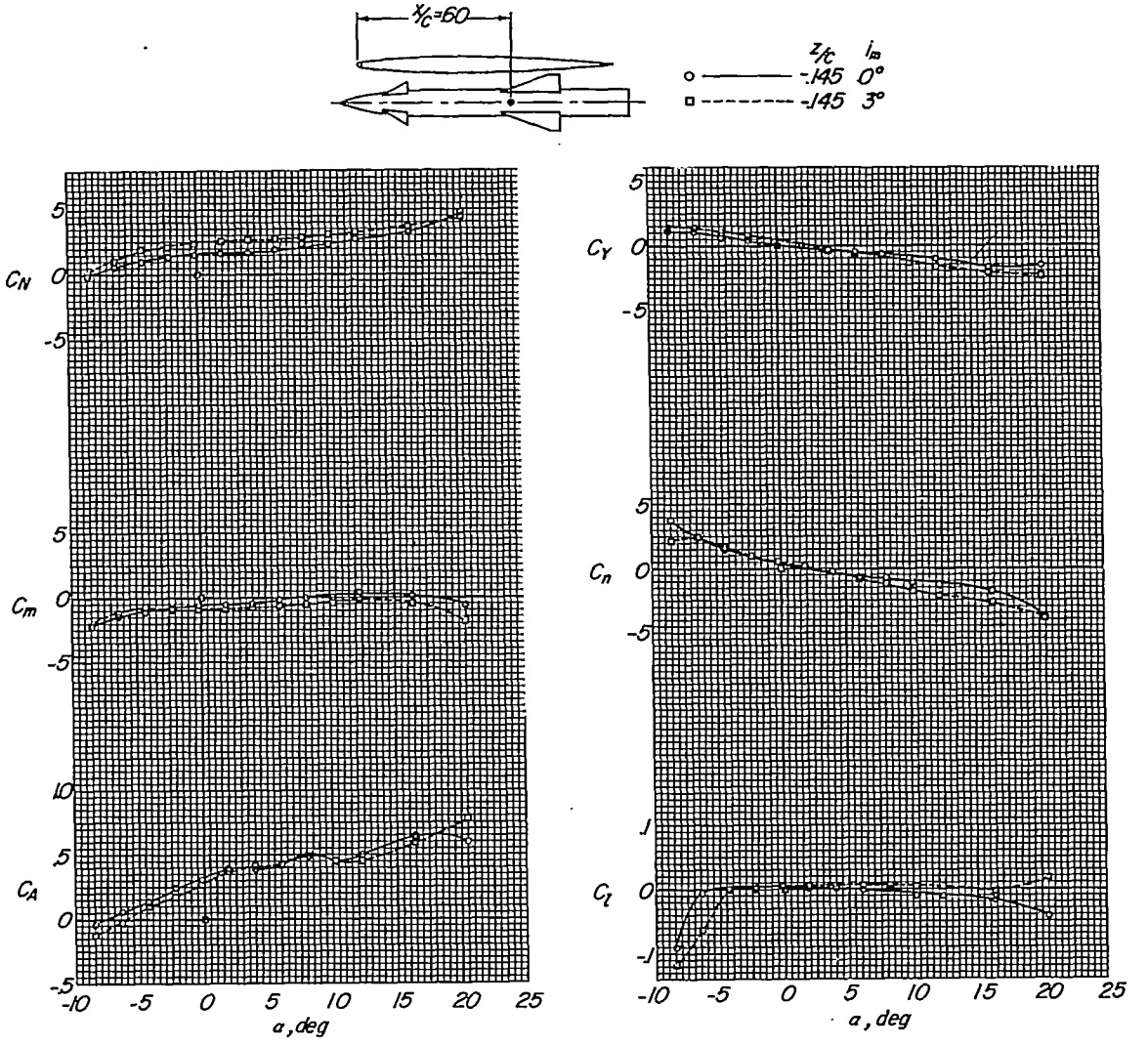

(a) x/c = 0.60.

Figure 7.- Effect of incidence on missile aerodynamic characteristics at one-half semispan station of wing-fuselage combination.

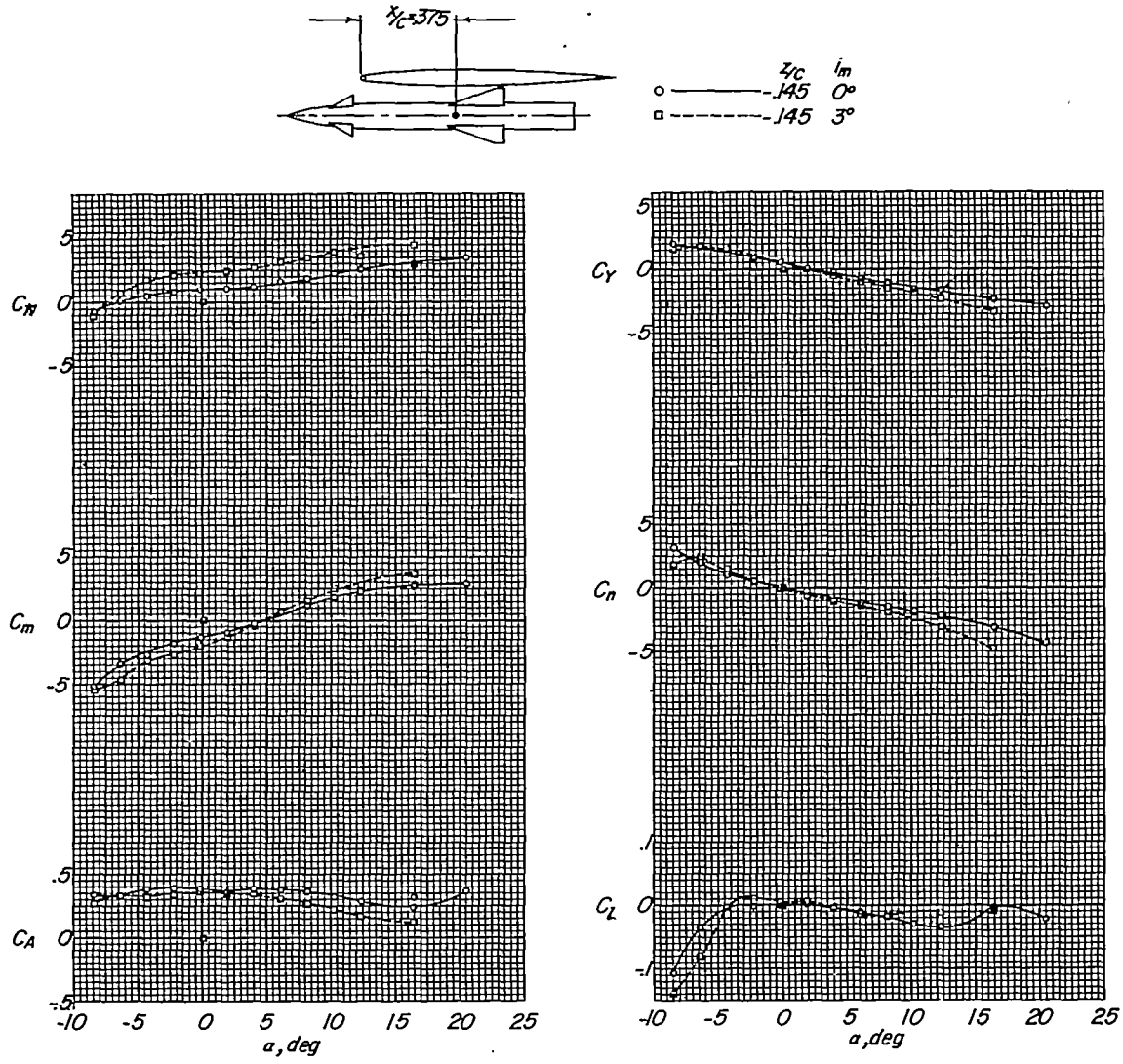

(b) x/c = 0.375.

Figure 7.- Continued.

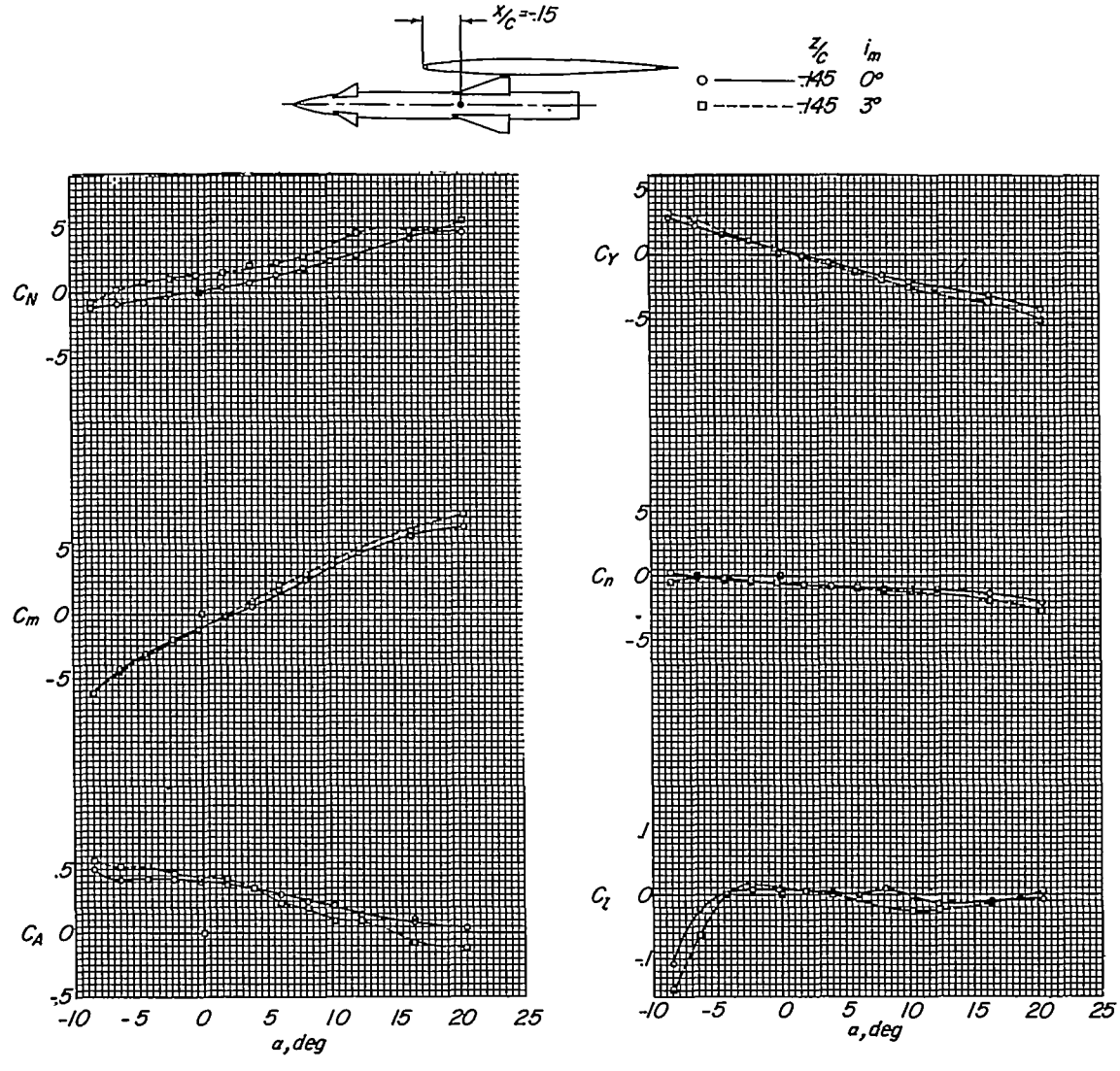

(c) x/c = -0.15.

Figure 7.- Continued.

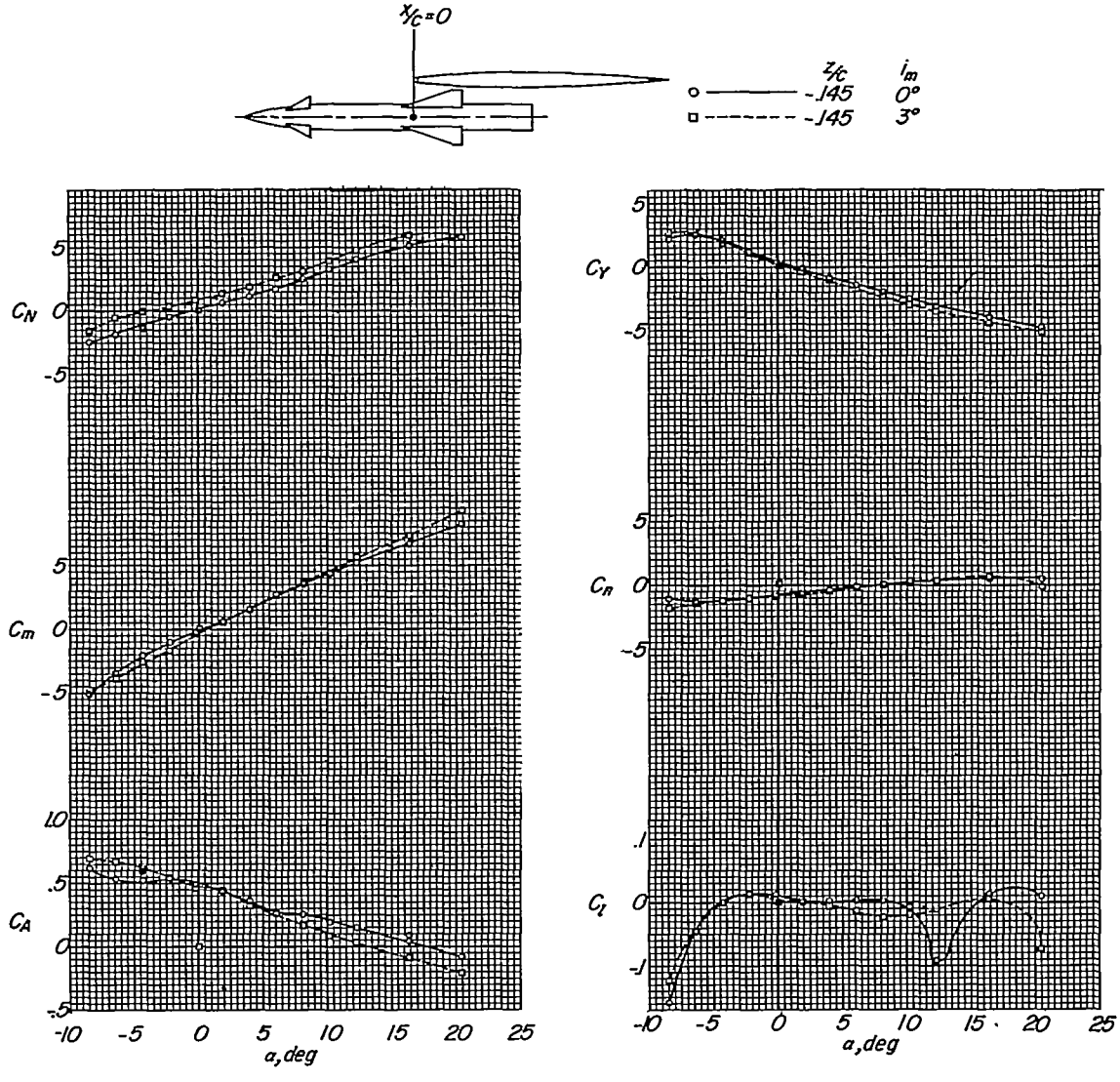

(d) x/c = 0.

Figure 7.- Continued.

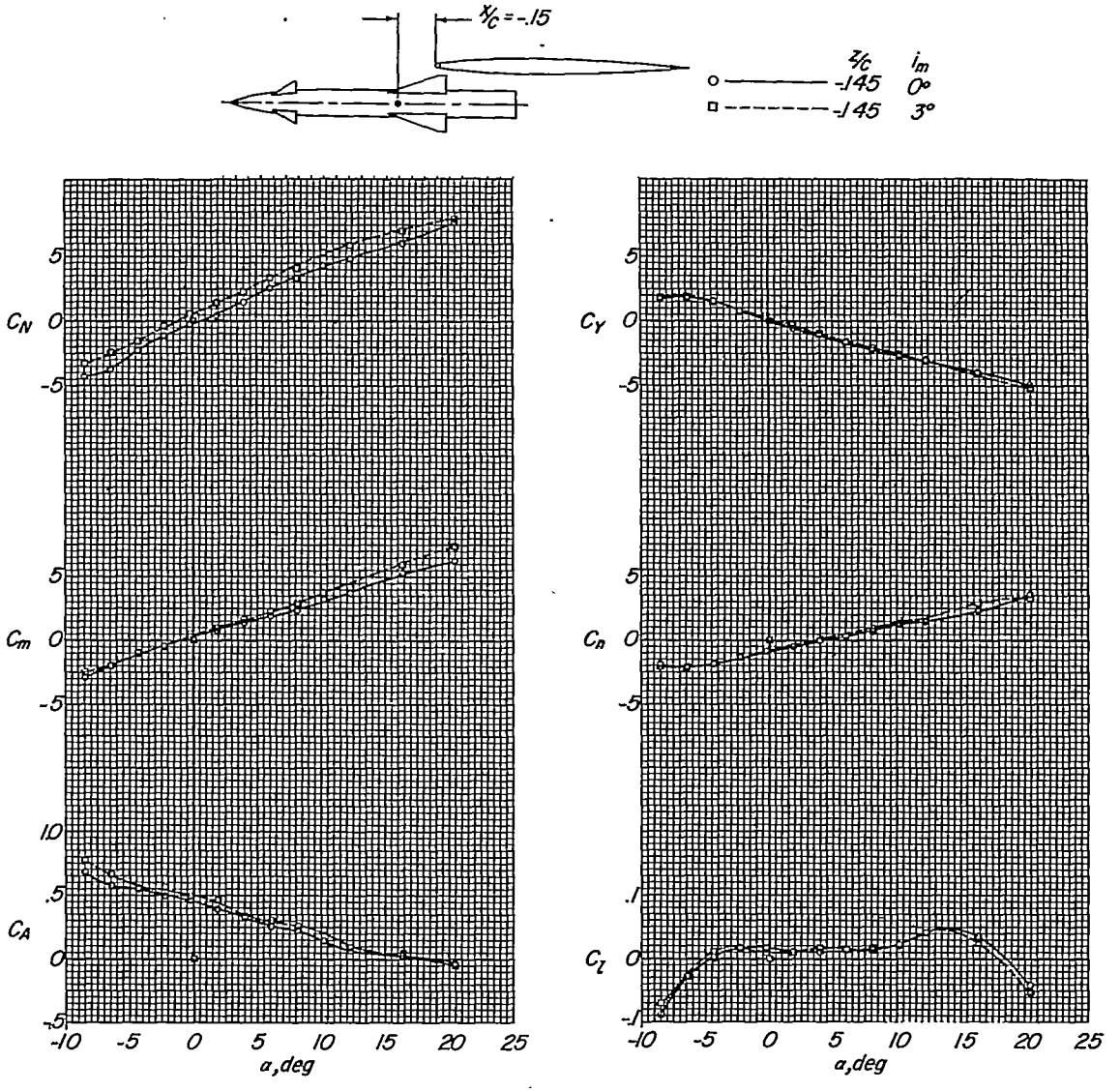

(e) x/c = -0.15.

Figure 7.- Concluded.

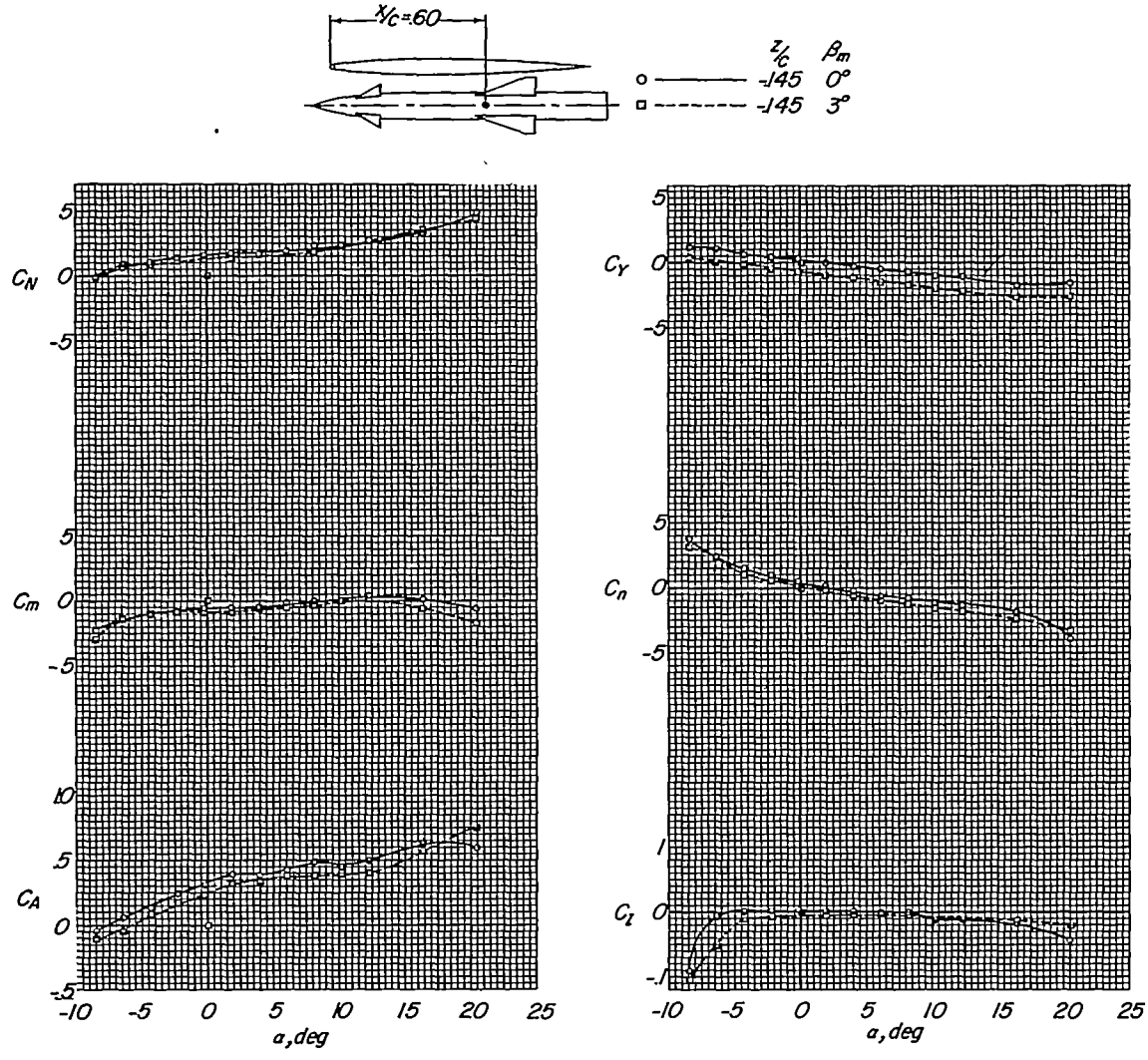

(a) x/c = 0.60.

Figure 8.- Effect of sideslip on missile aerodynamic characteristics at one-half semispan station of wing-fuselage combination.

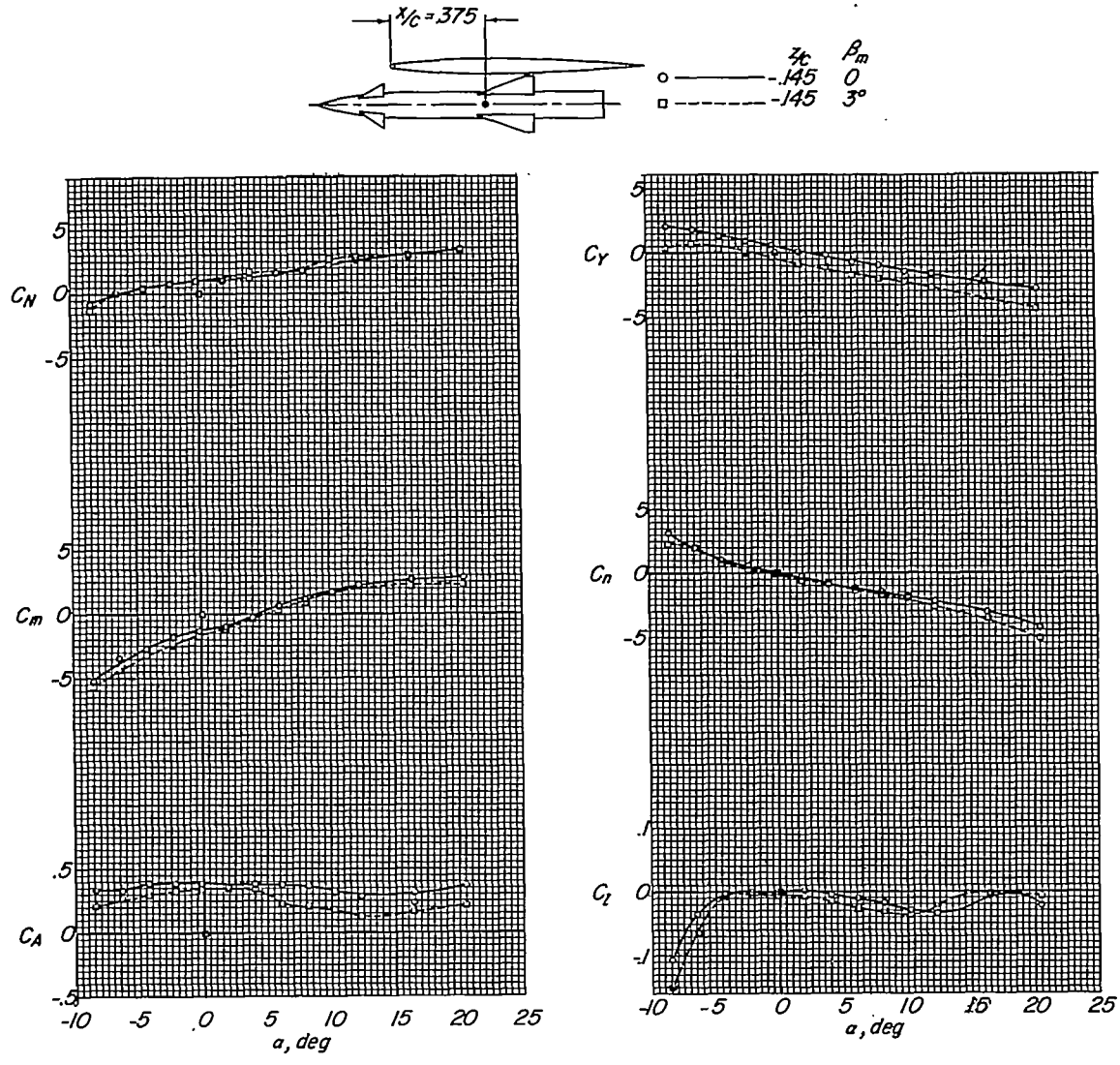

(b) x/c = 0.375.

Figure 8.- Continued.

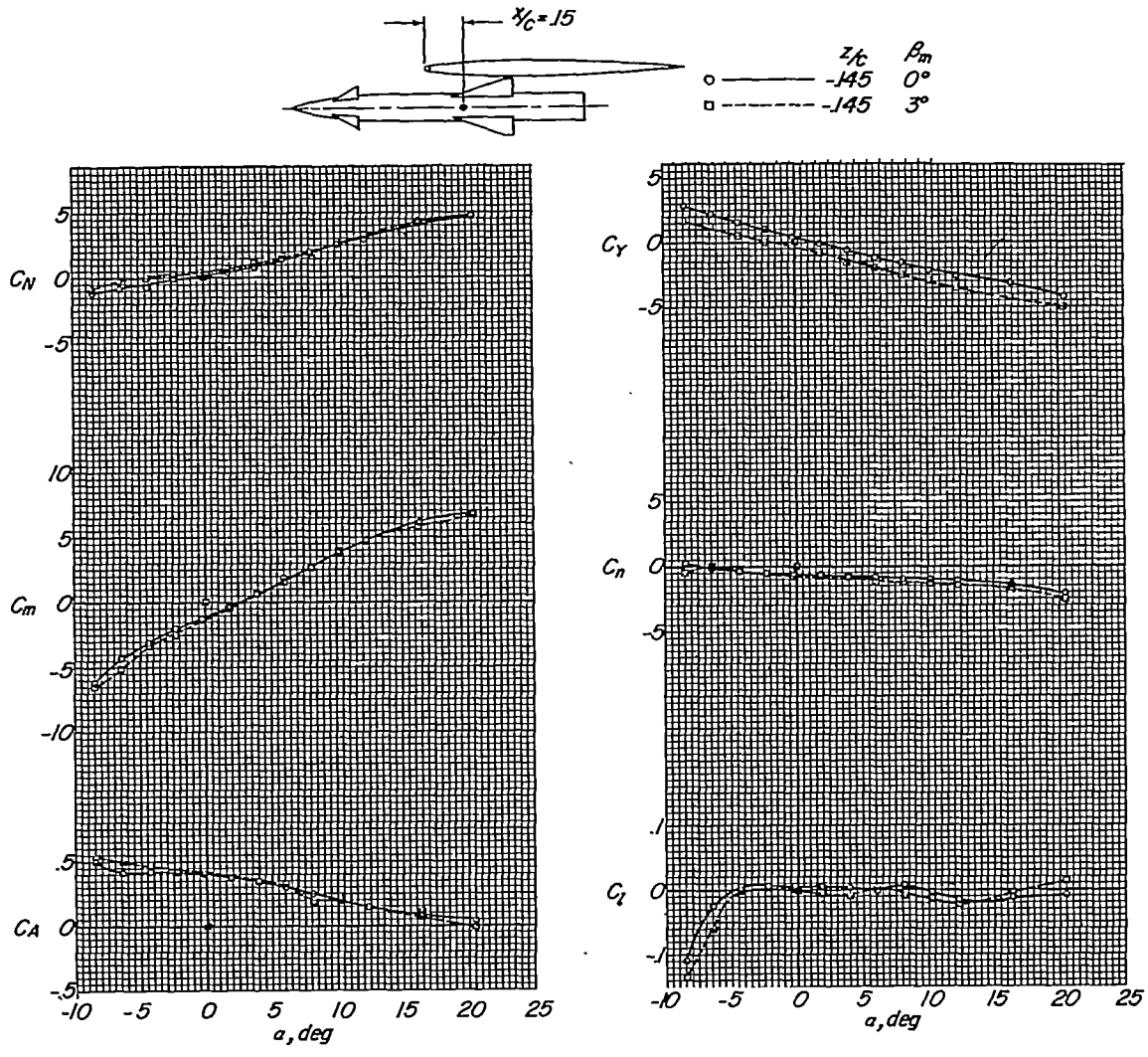

(c) x/c = 0.15.

Figure 8.- Continued.

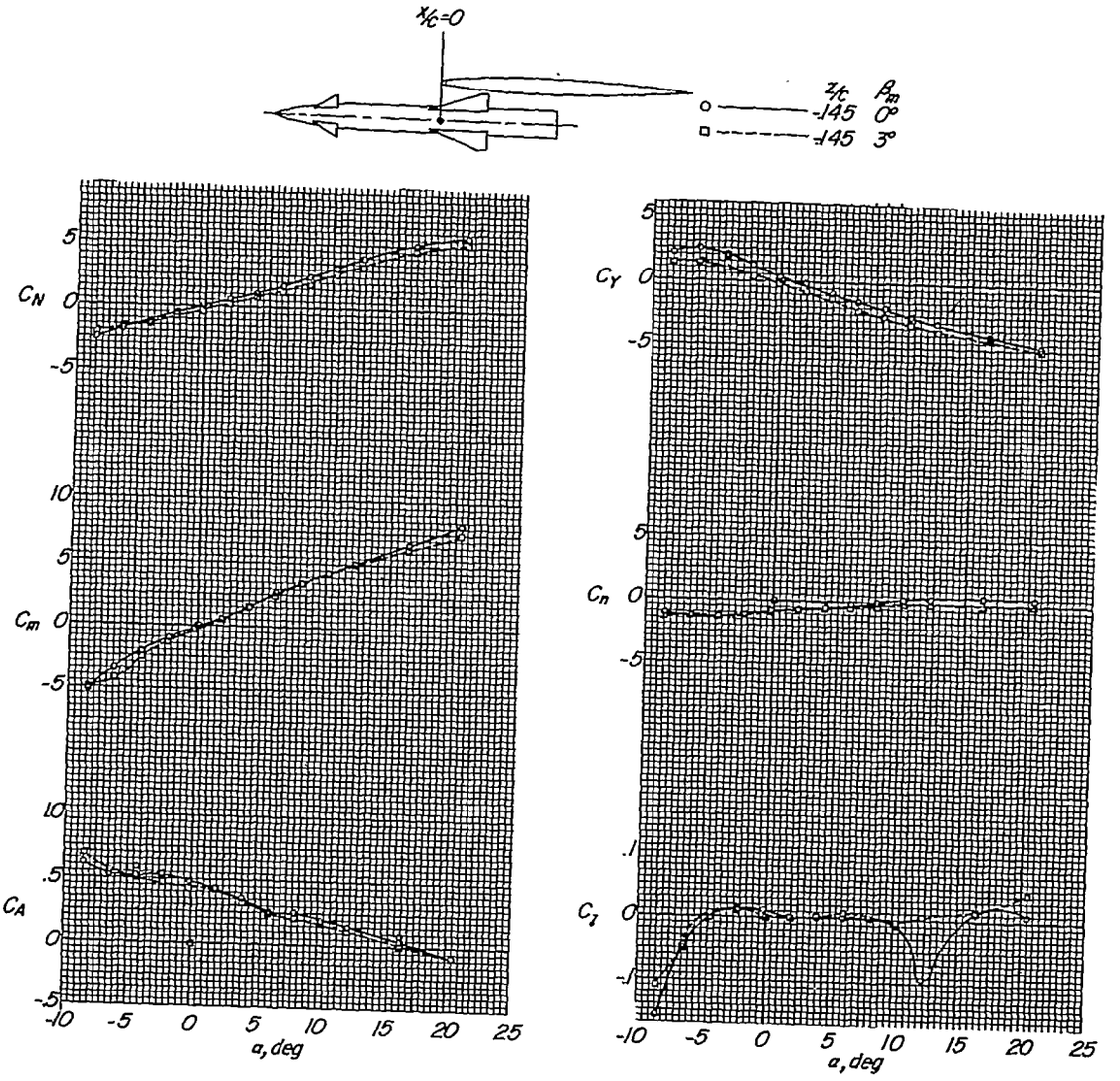

(d) x/c = 0.

Figure 8.- Continued.

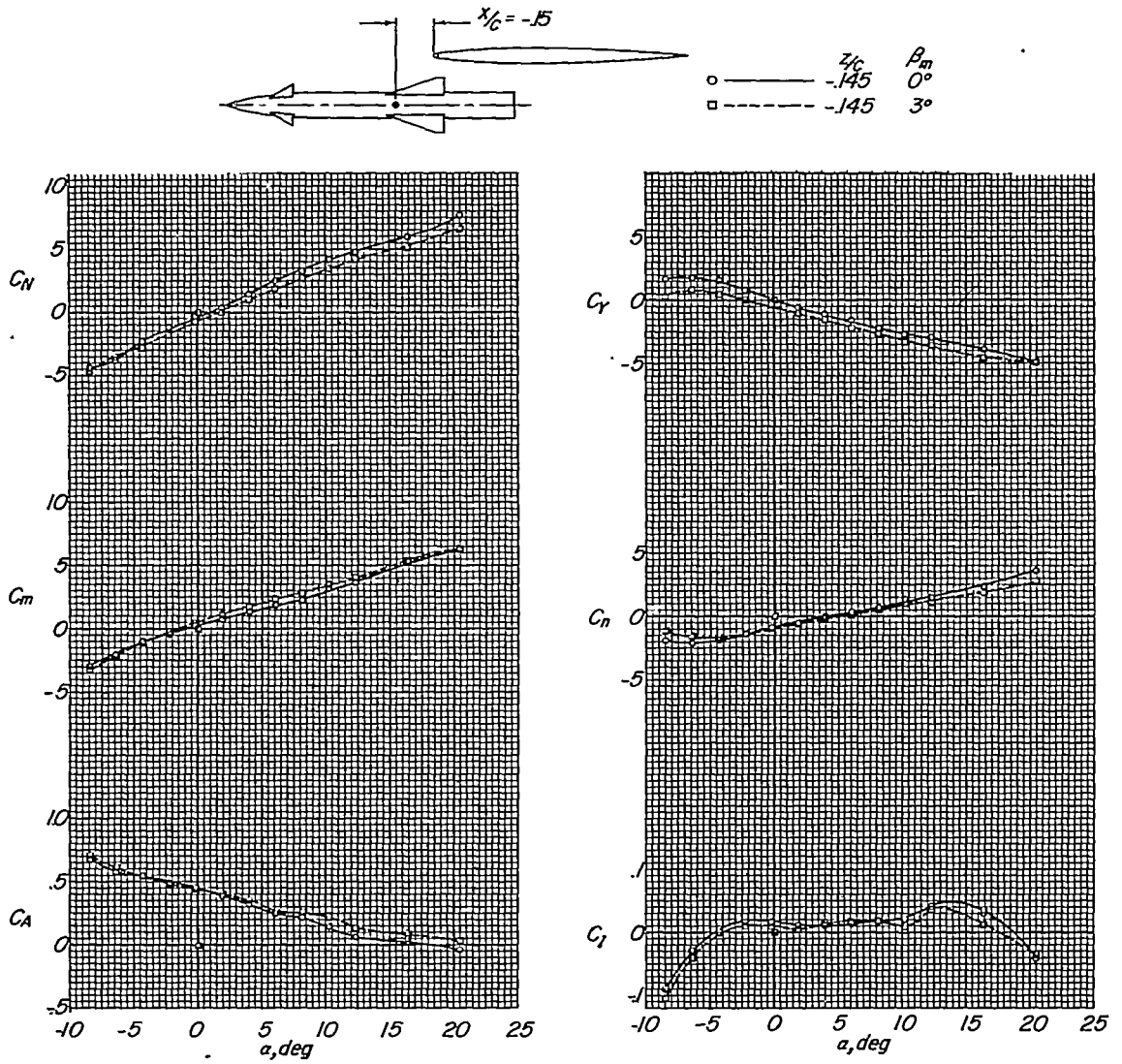

(e) x/c = -0.15.

Figure 8.- Concluded.

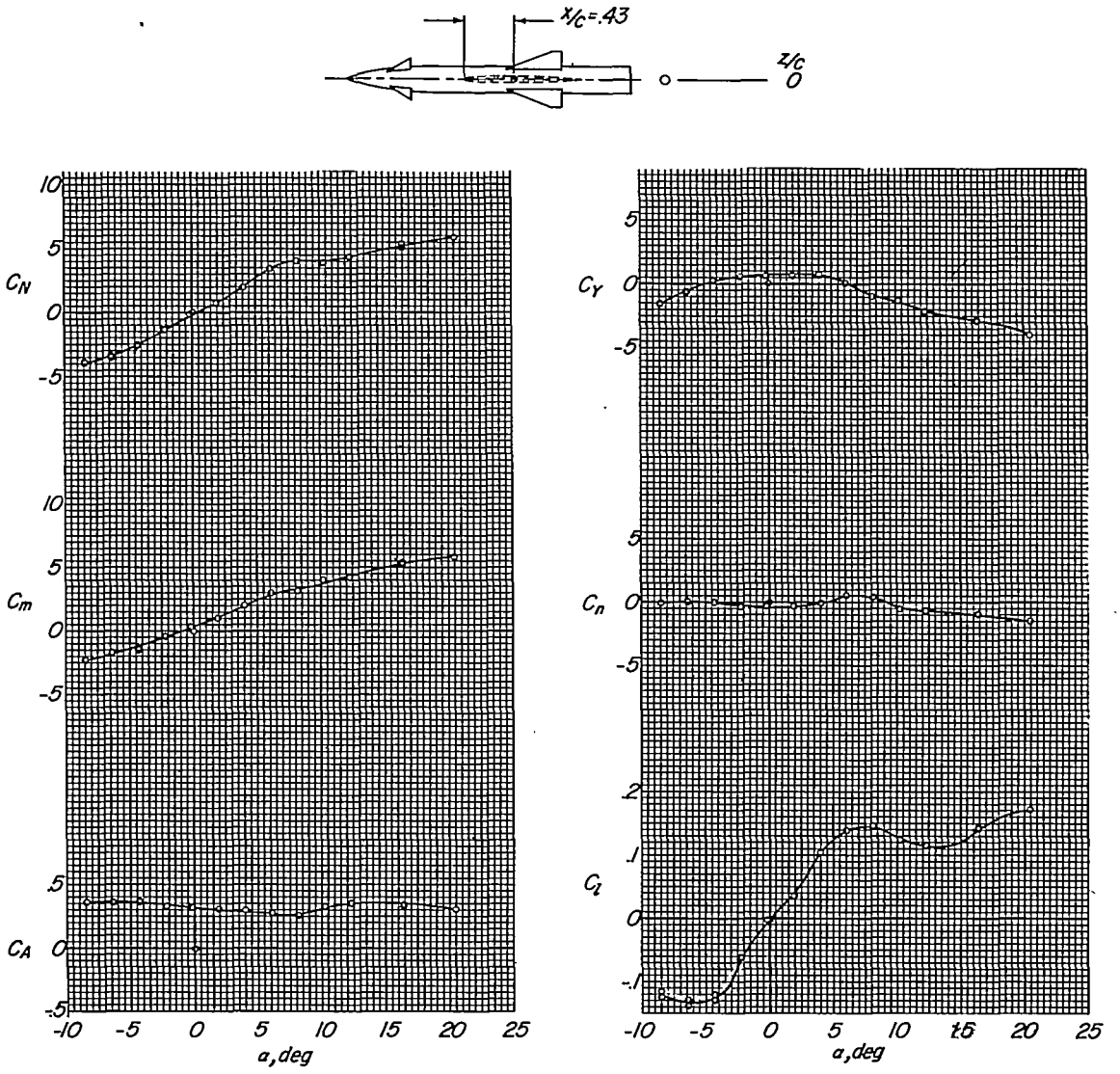

(a) x/c = 0.43.

Figure 9.- Missile aerodynamic characteristics at wing-tip location of wing-fuselage combination.

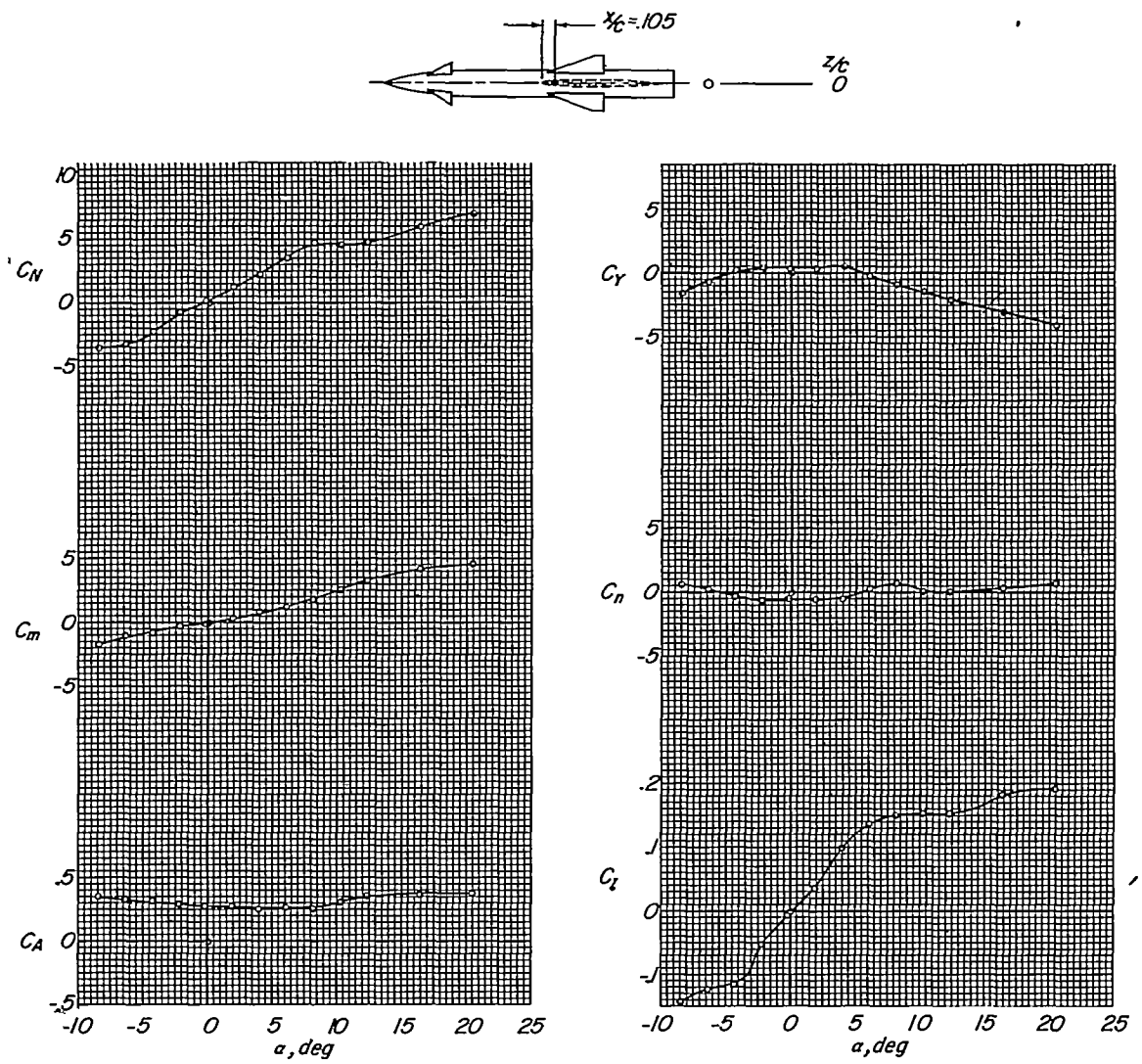

(b) x/c = 0.105.

Figure 9.- Continued.

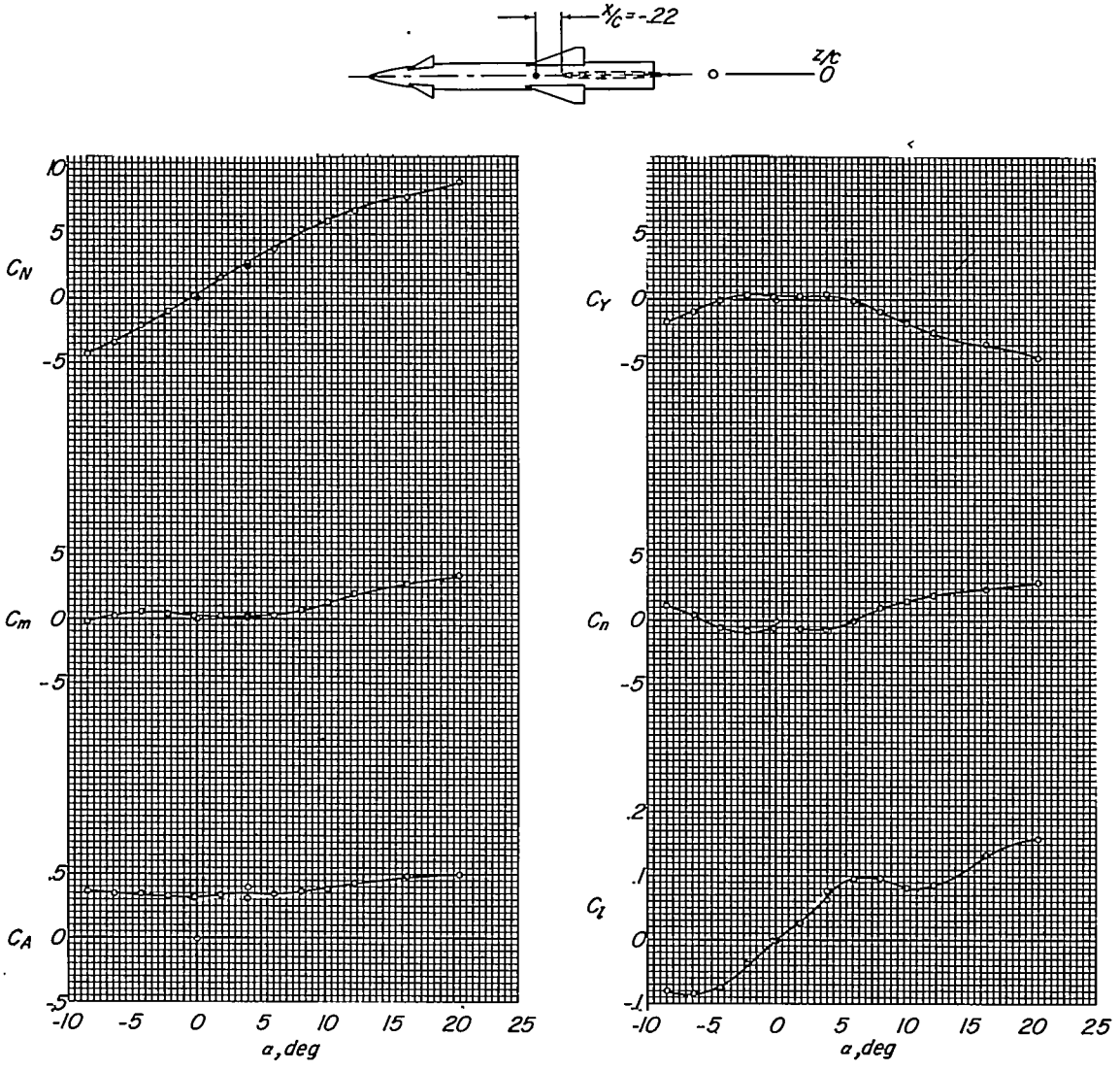

(c) x/c = -0.22.

Figure 9.- Continued.

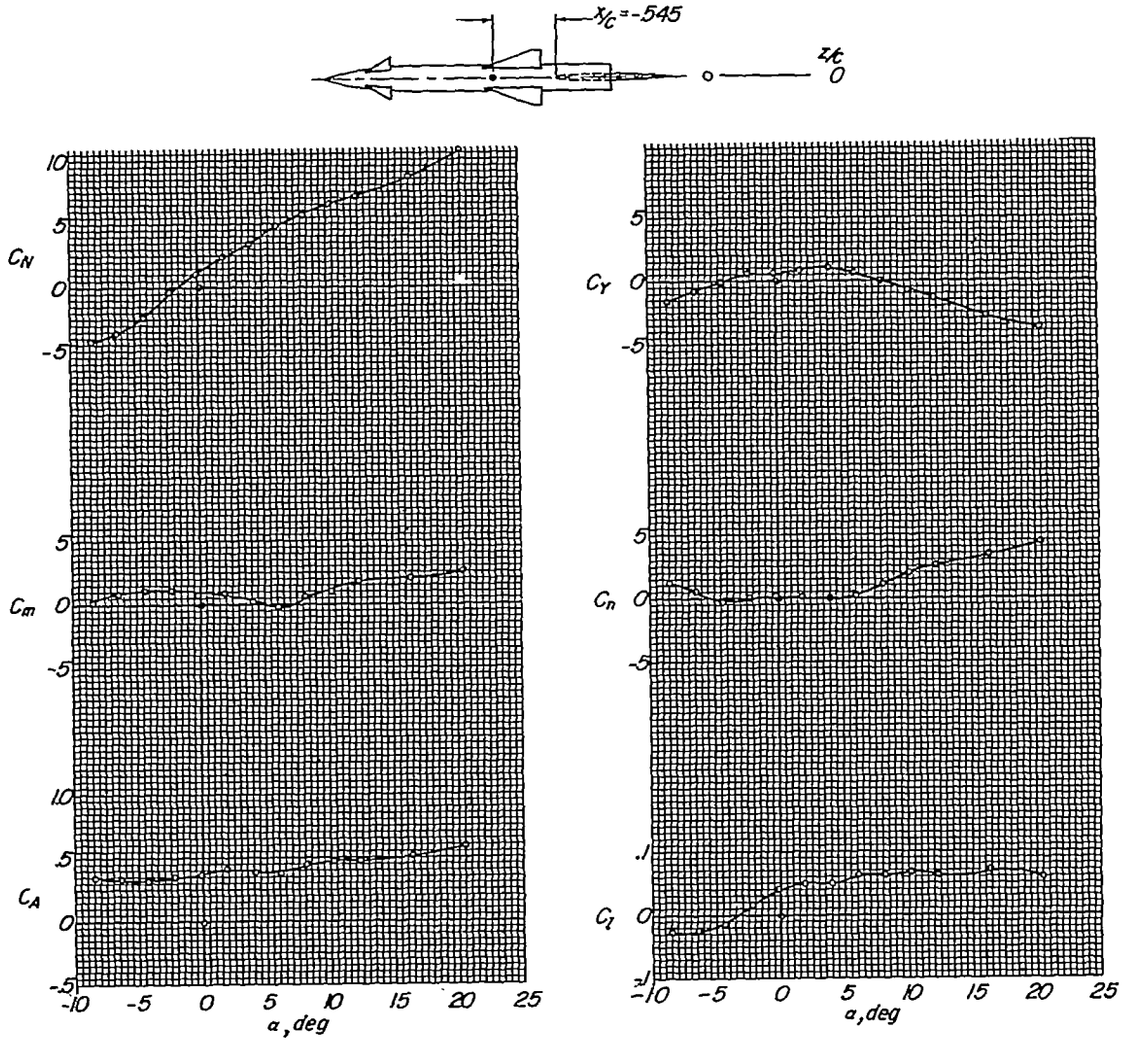

(d) x/c = -0.545.

Figure 9.- Continued.

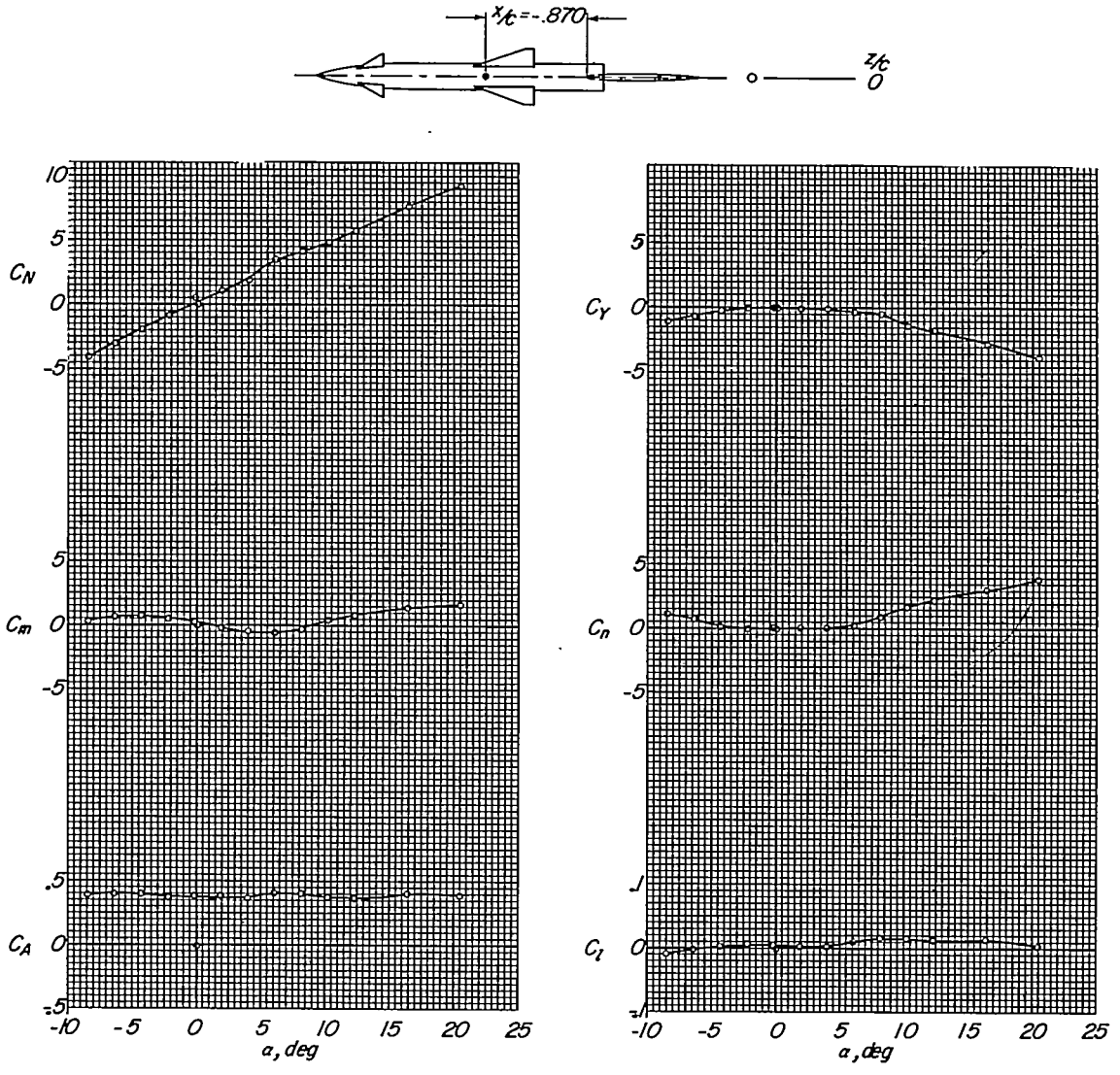

(e) x/c = -0.870.

Figure 9.- Continued.

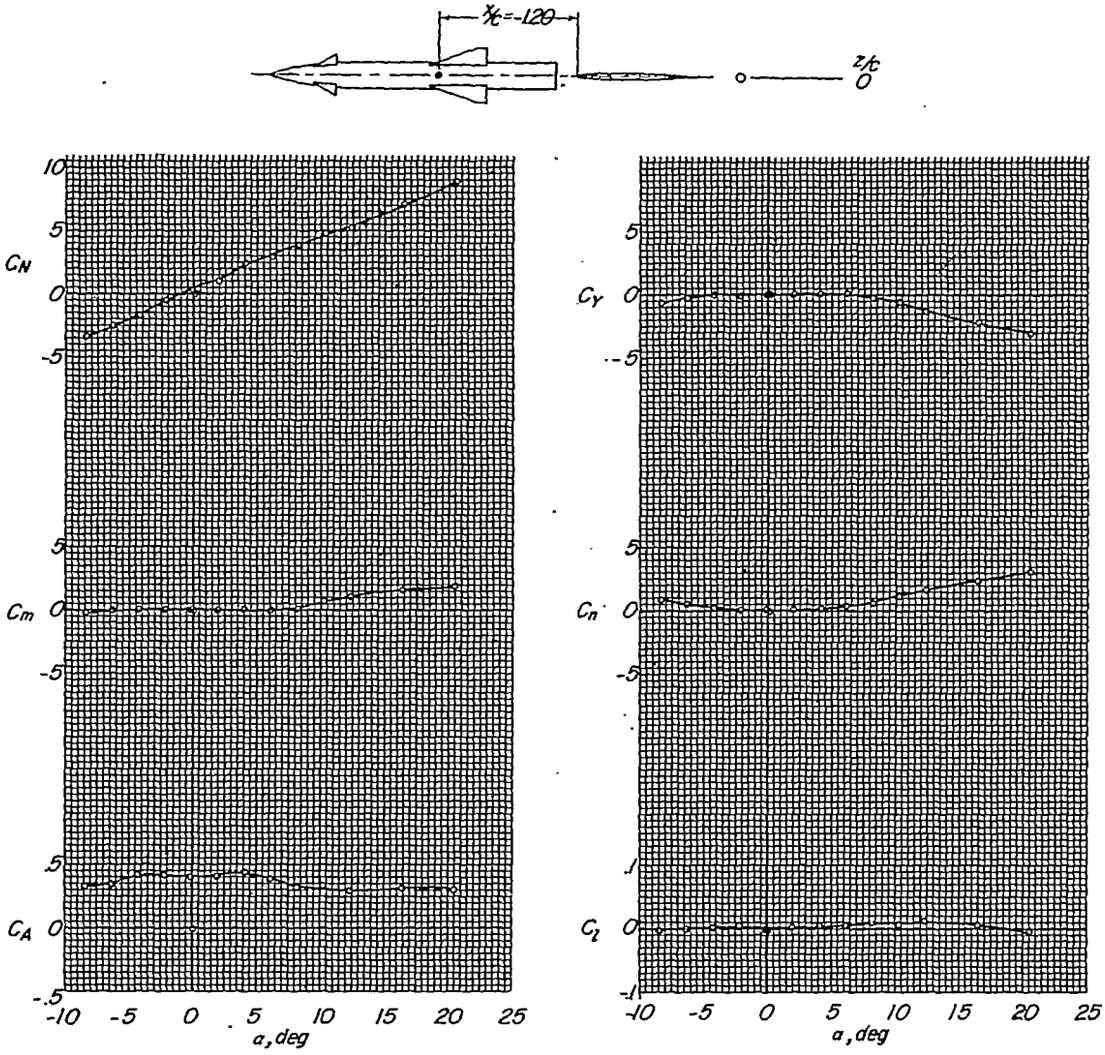

(f) x/c = -1.20.

Figure 9.- Continued.

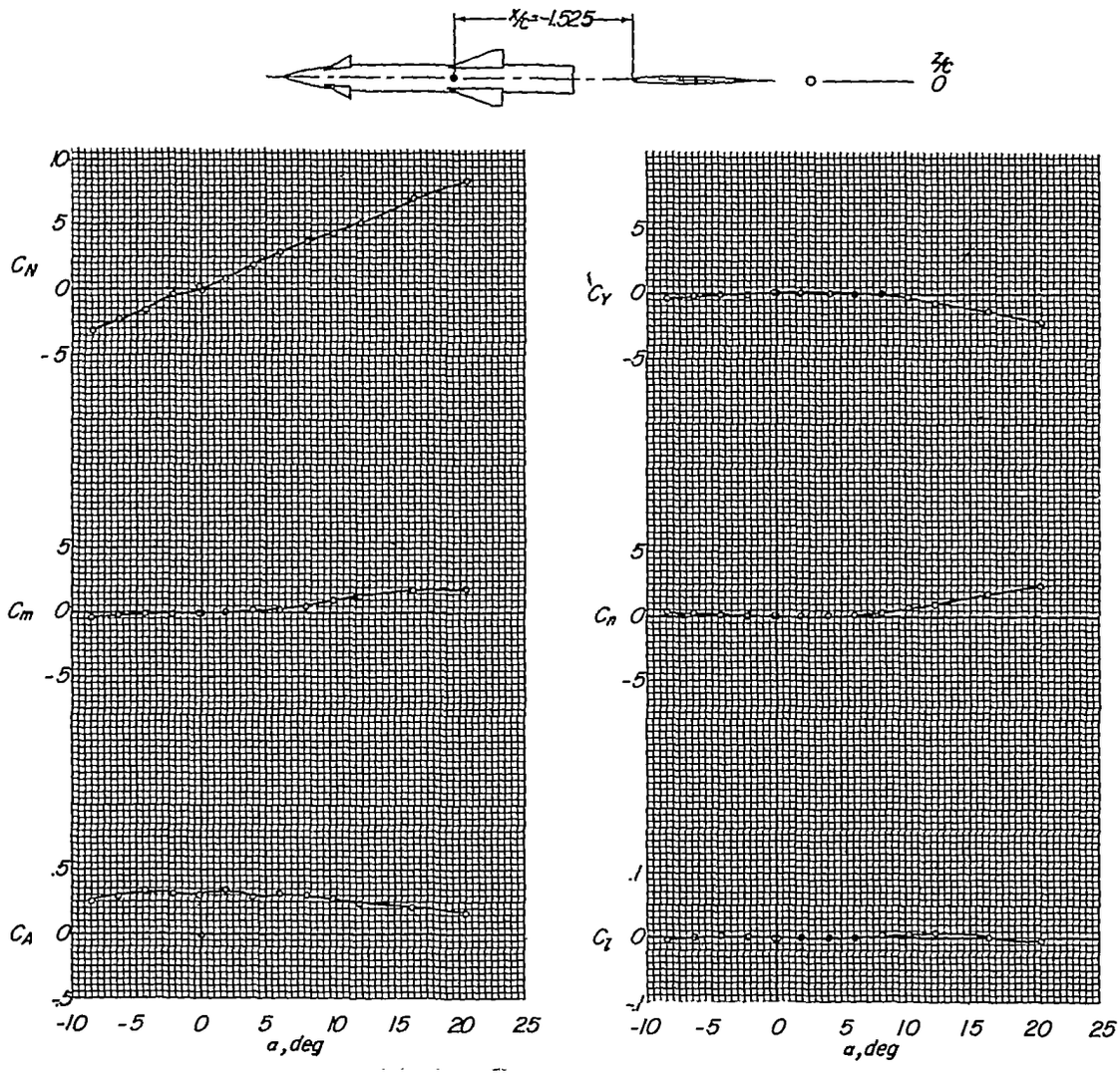

(g) x/c = -1.525.

Figure 9.- Concluded.

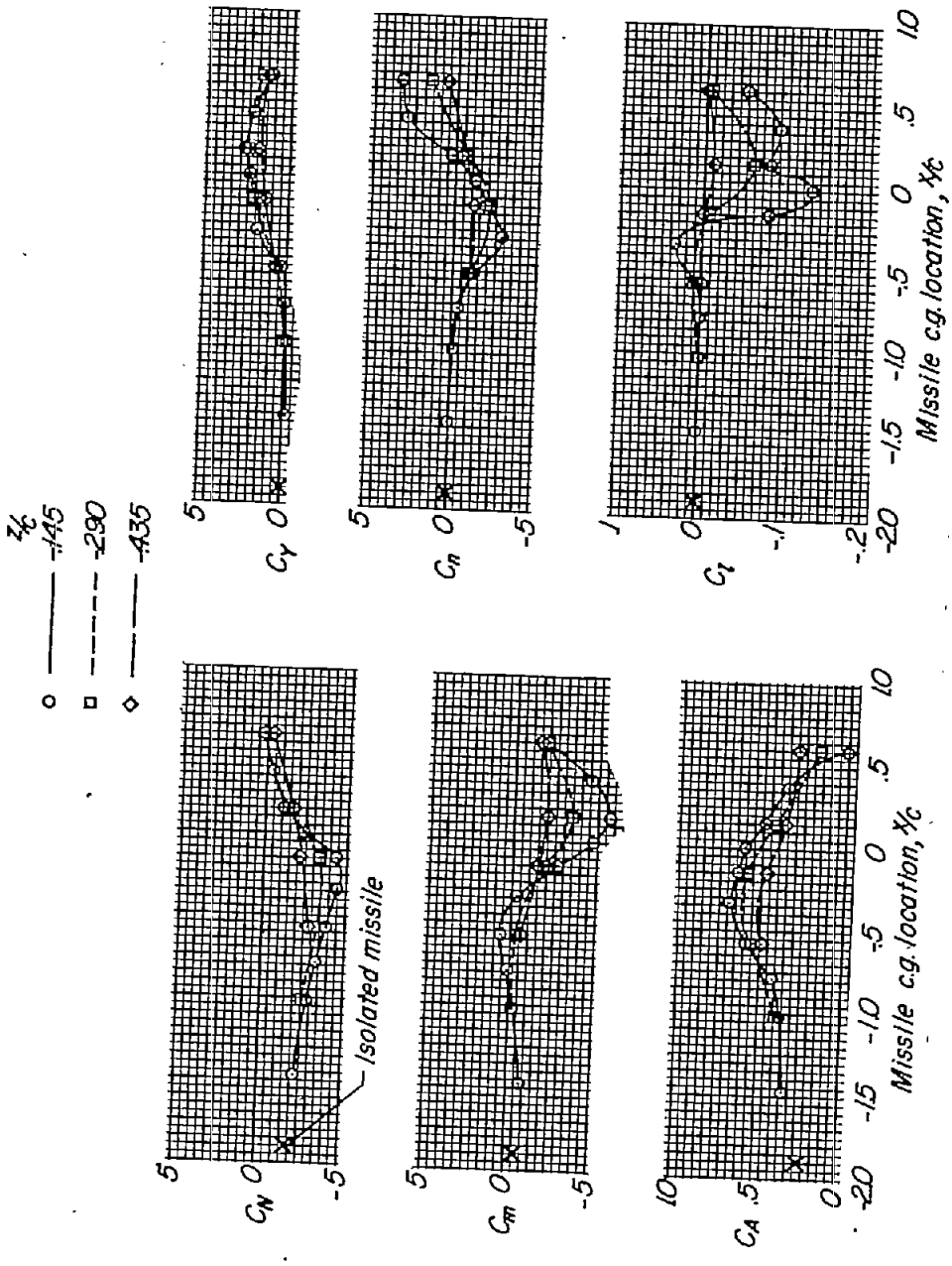

(a) $\alpha = -8^\circ$.

Figure 10.- Chordwise summary of missile static aerodynamic characteristics at one-half semispan location.

CONFIDENTIAL

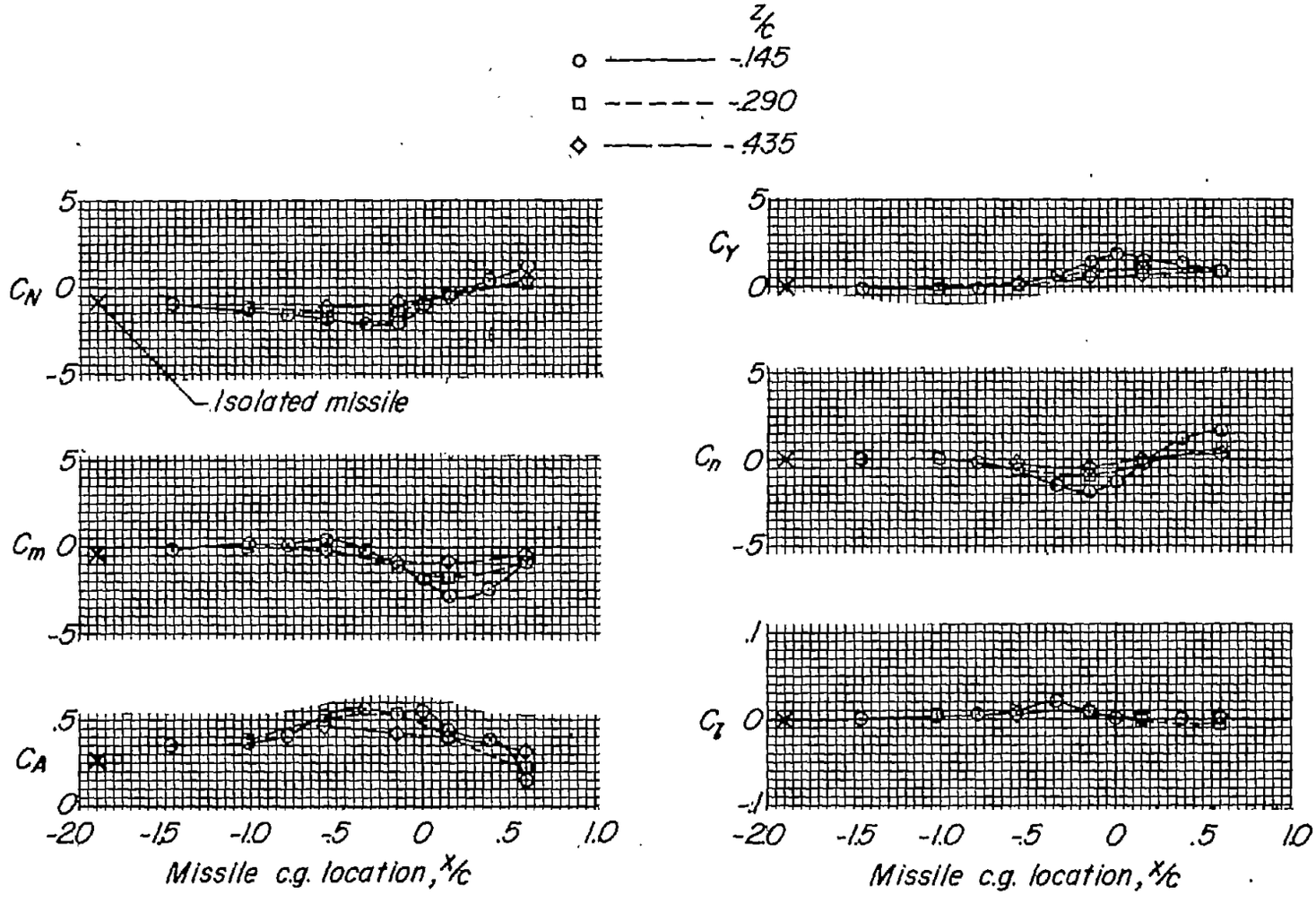

(b) $\alpha = -4^\circ$.

Figure 10.- Continued.

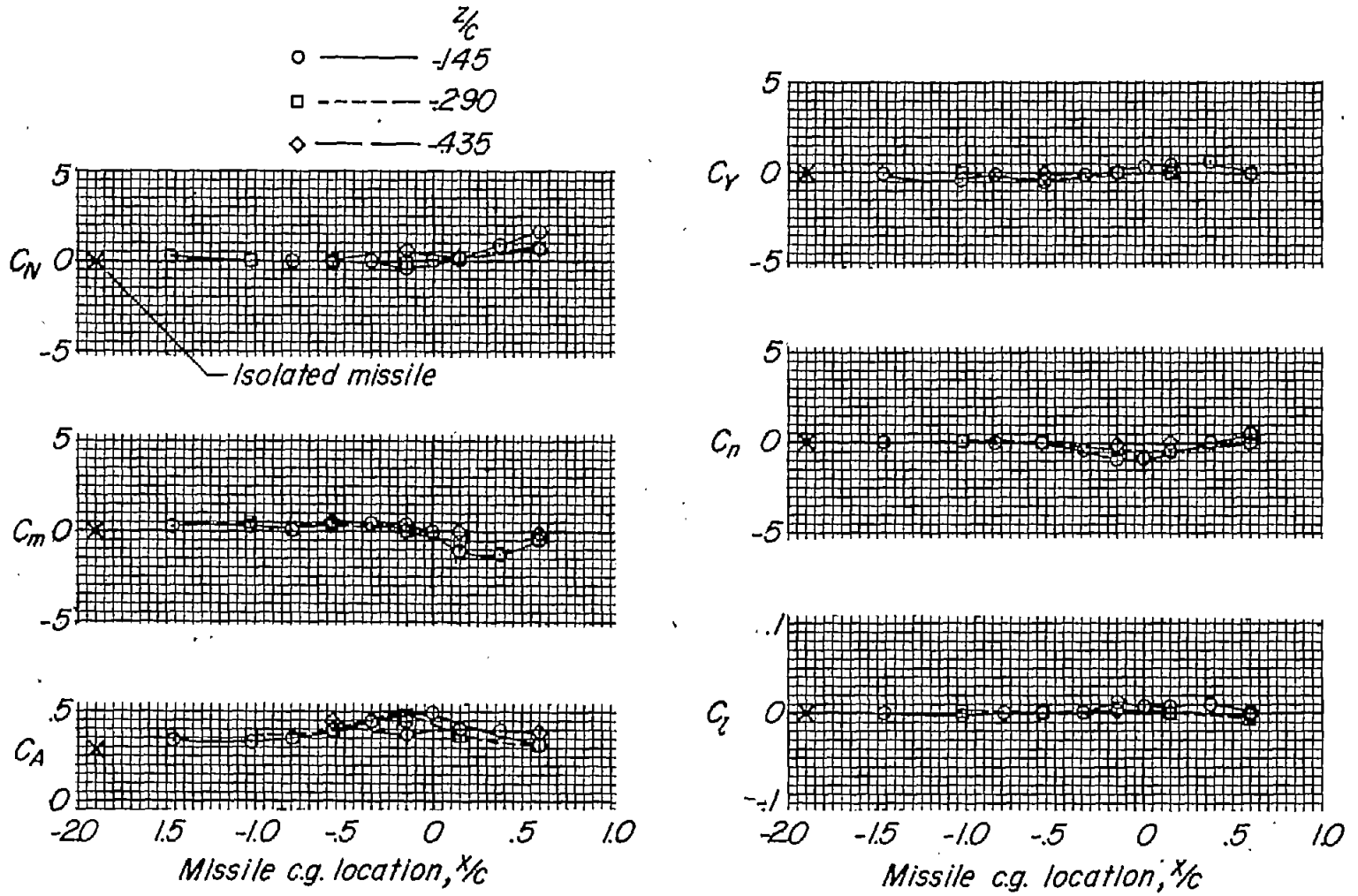

(c) $\alpha = 0^\circ$.

Figure 10.- Continued.

CONFIDENTIAL

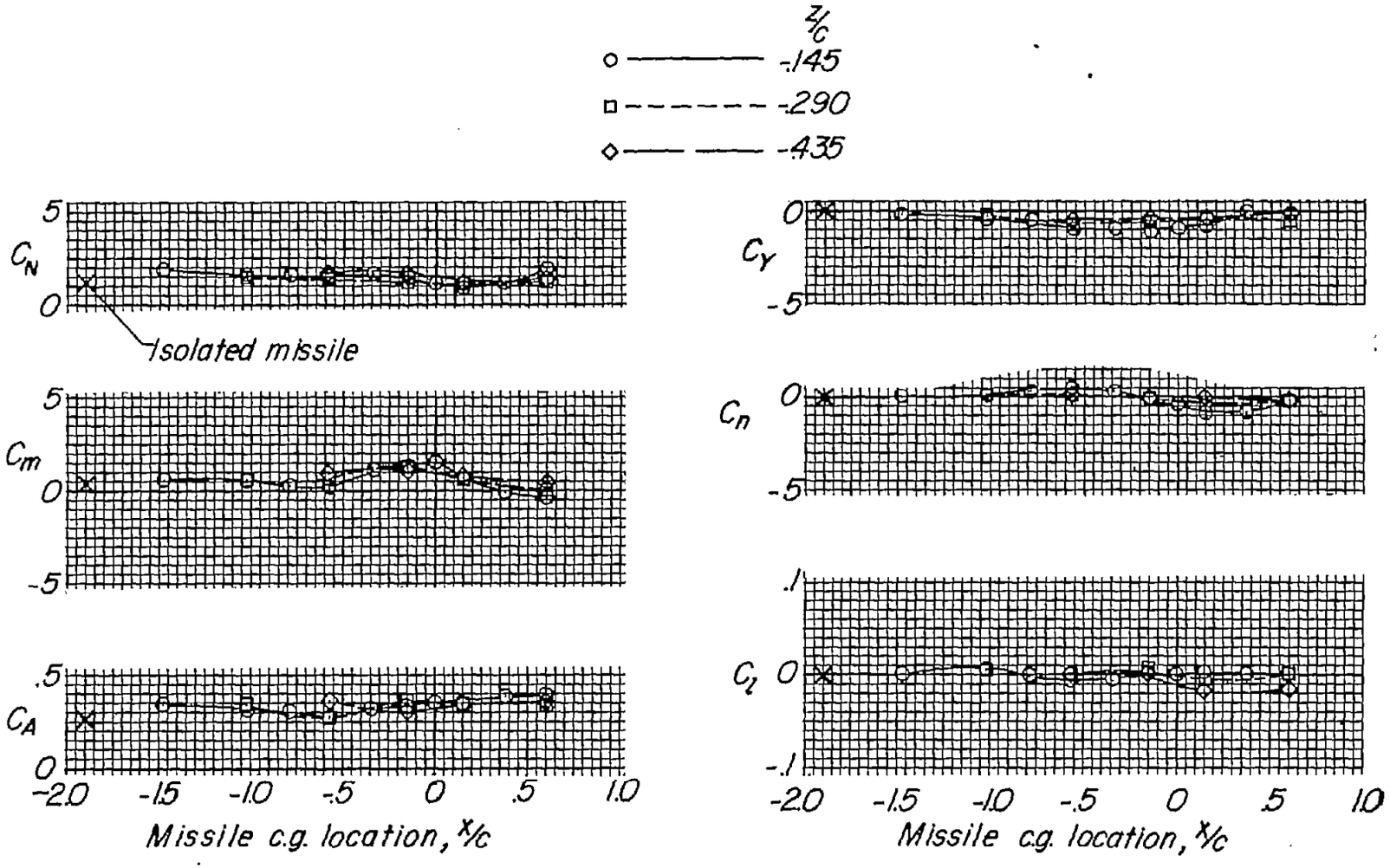

(d) $\alpha = 4^\circ$.

Figure 10.- Continued.

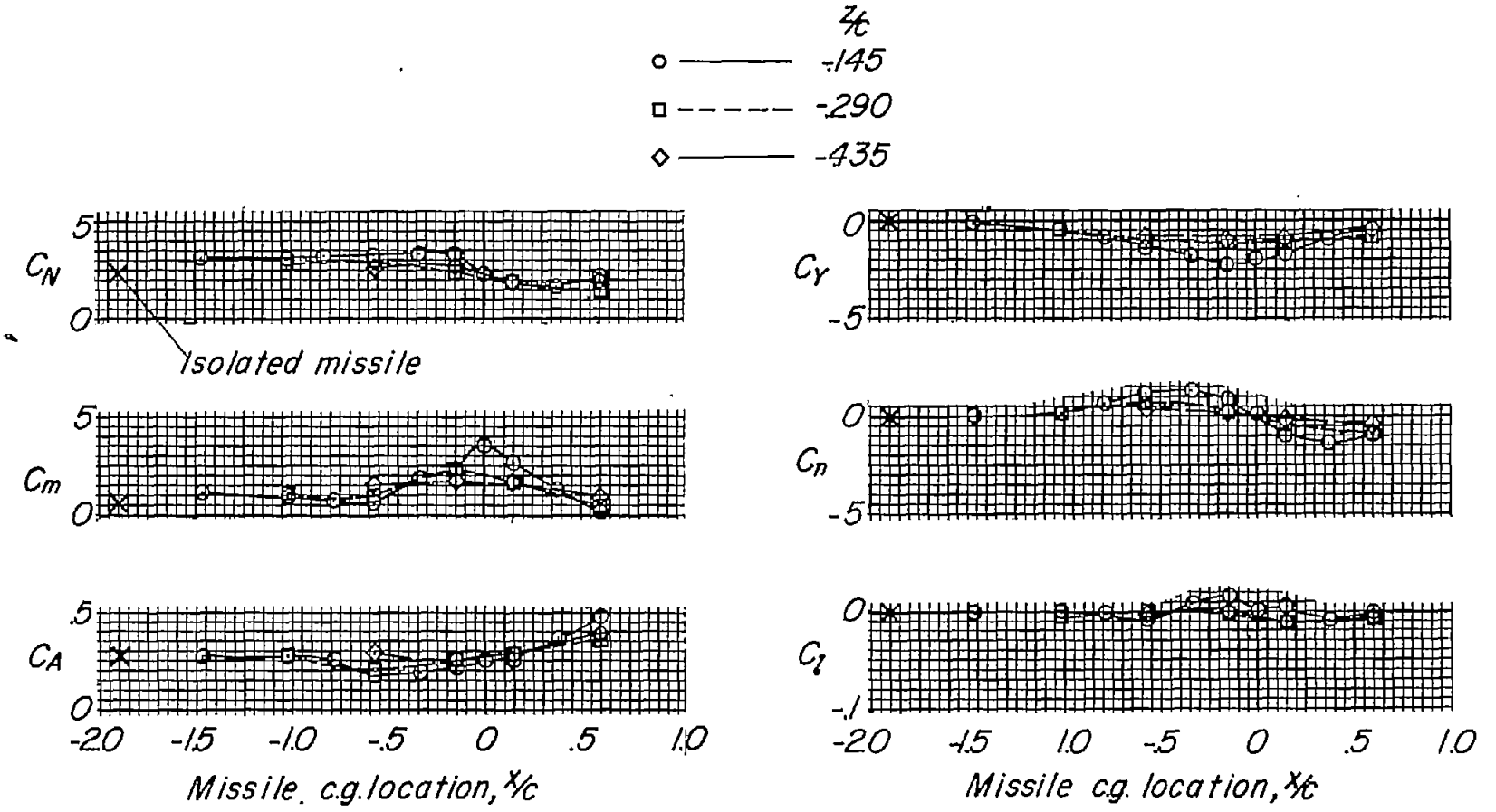

(e) $\alpha = 8^\circ$.

Figure 10.- Continued.

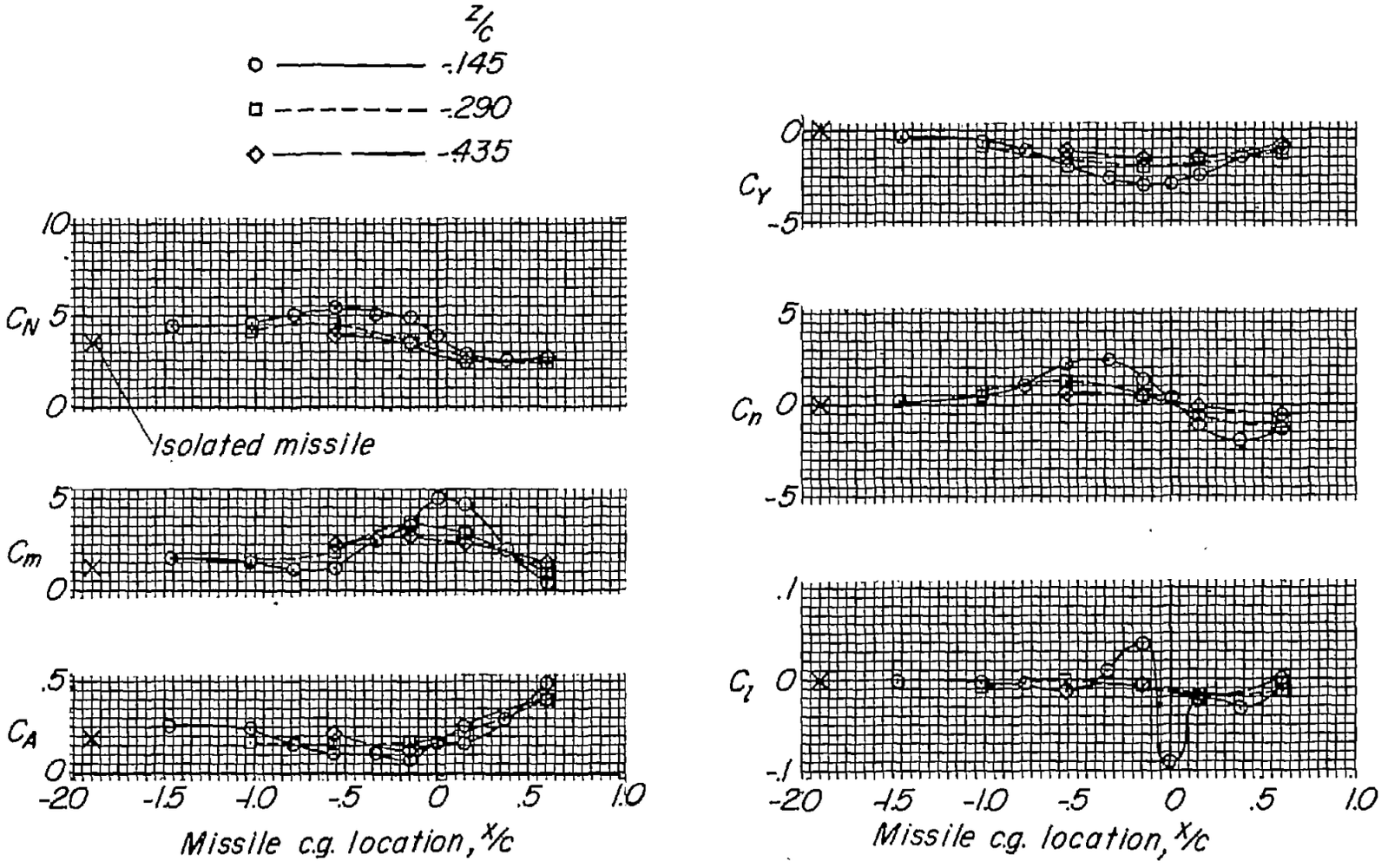

(f) $\alpha = 12^\circ$.

Figure 10.- Continued.

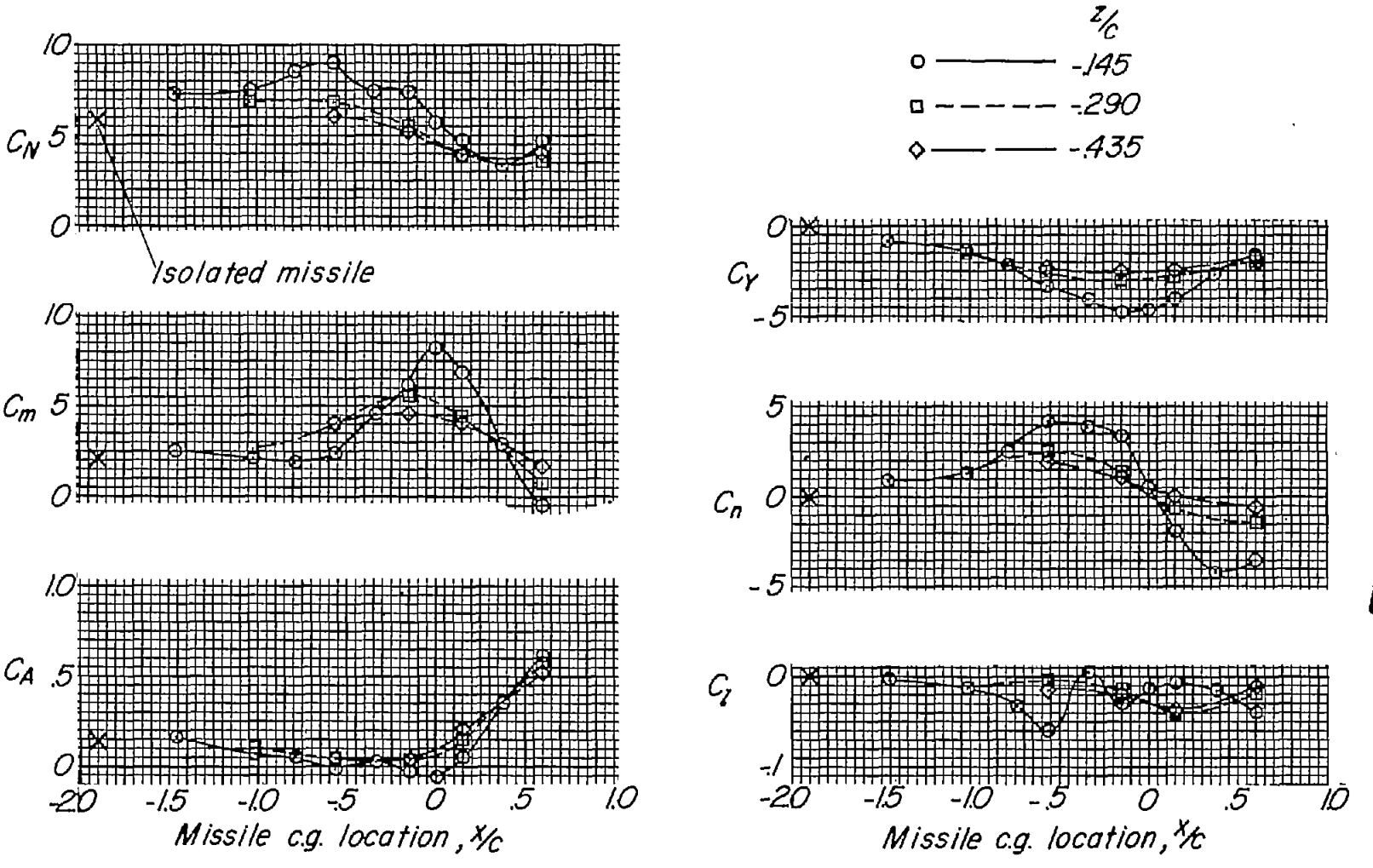

(g) $\alpha = 20^\circ$.

Figure 10.- Concluded.

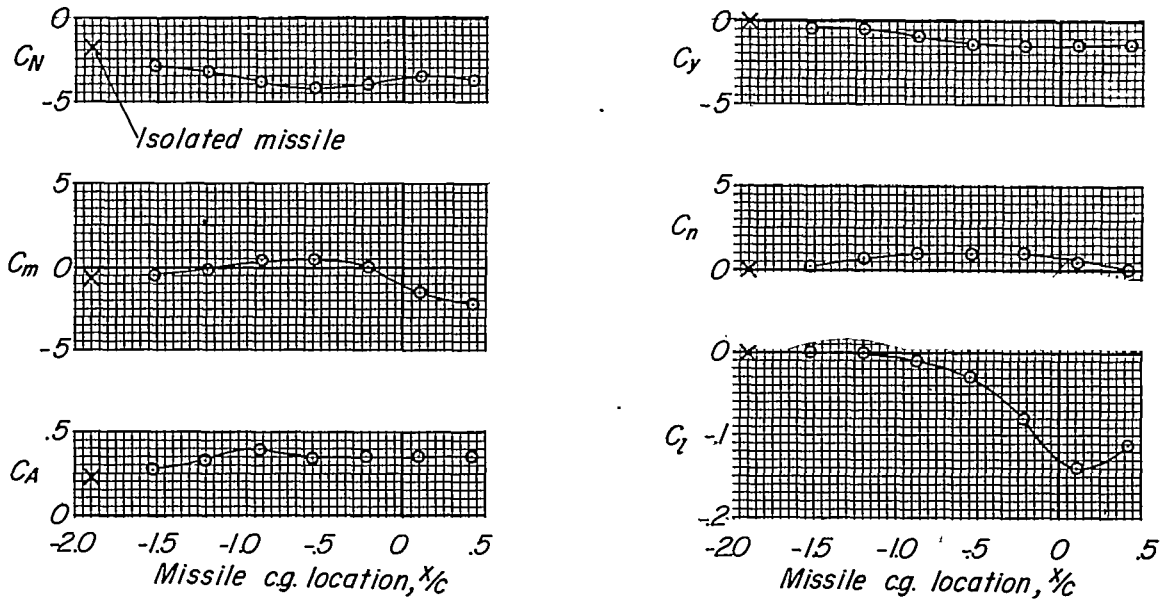

(a) $\alpha = -8^\circ$.

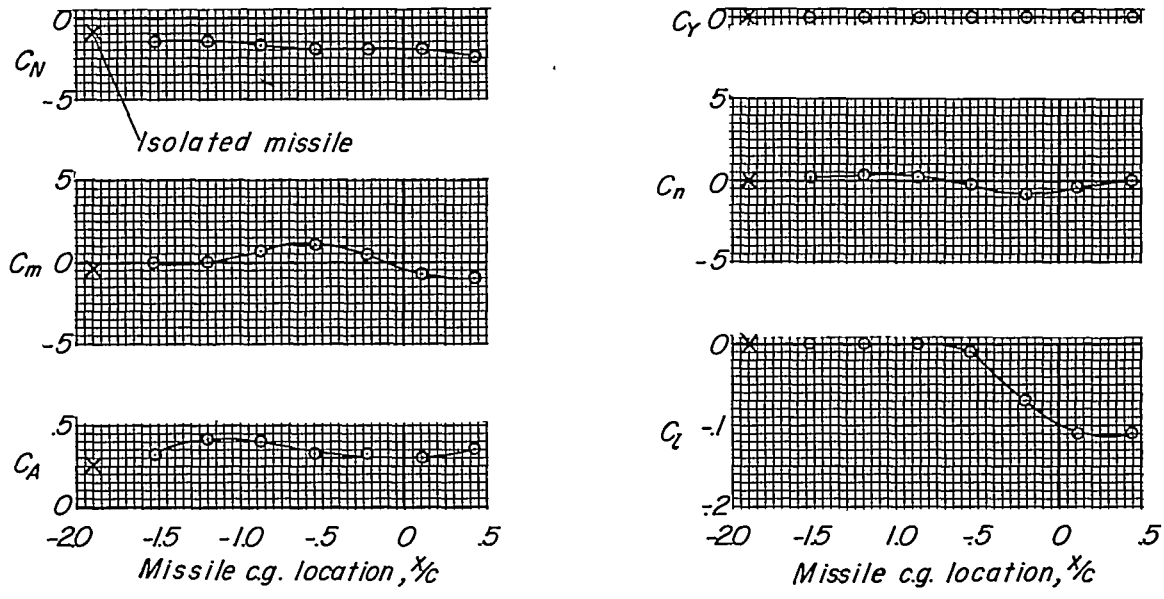

(b) $\alpha = -4^\circ$.

Figure 11.- Chordwise summary of missile static aerodynamic characteristics located at wing tip.

CONFIDENTIAL

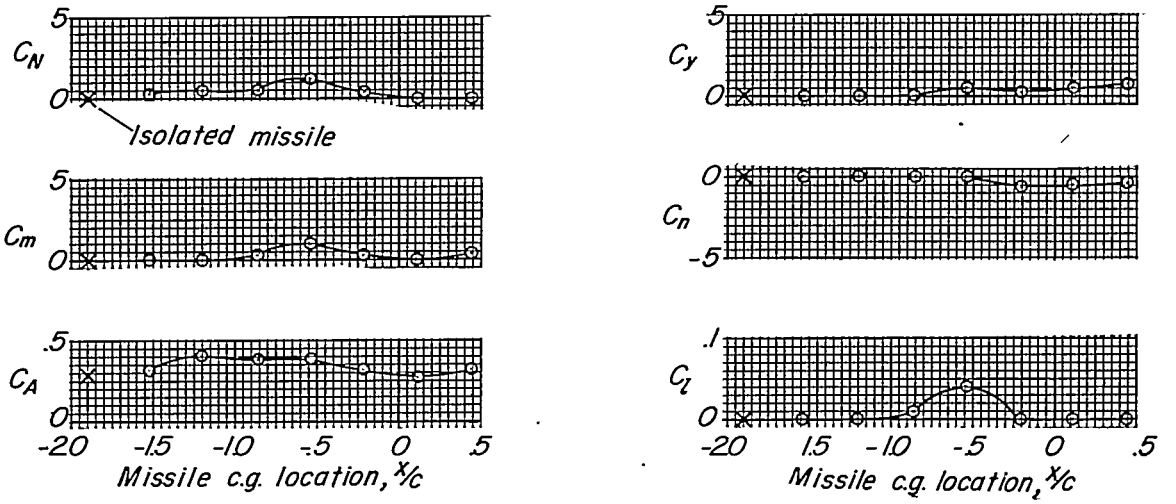

(c) $\alpha = 0^\circ$.

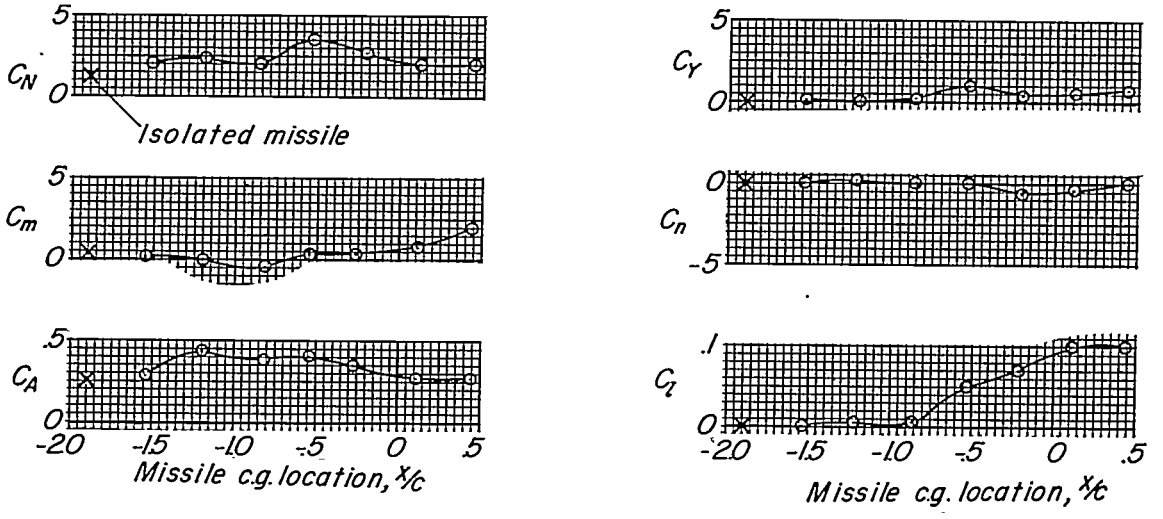

(d) $\alpha = 4^\circ$.

Figure 11.- Continued.

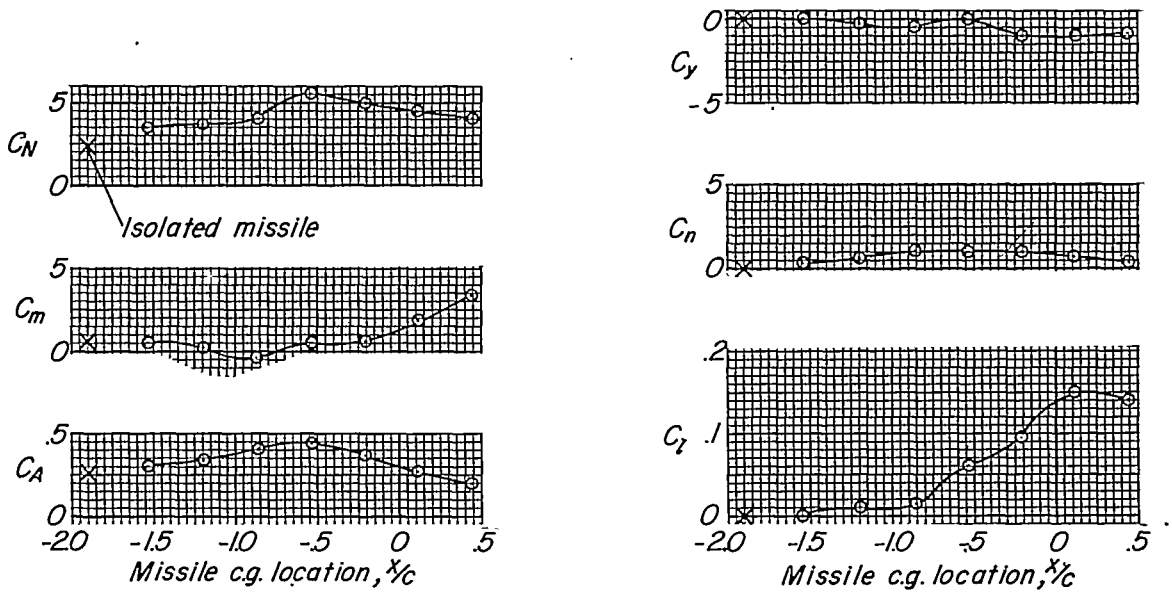

(e) $\alpha = 8^\circ$.

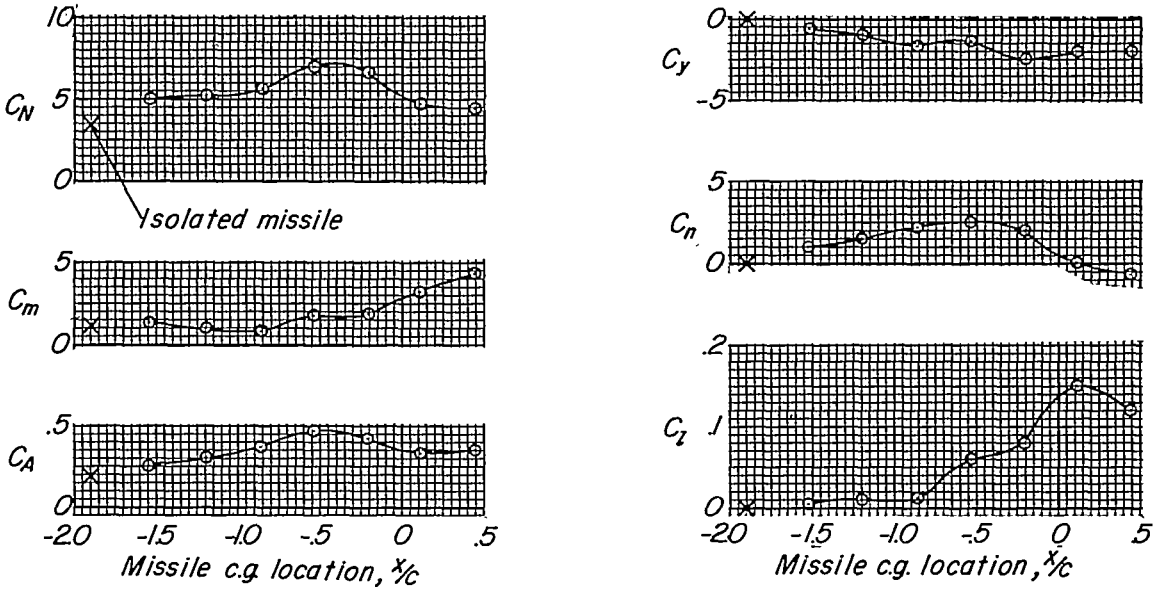

(f) $\alpha = 12^\circ$.

Figure 11.- Continued.

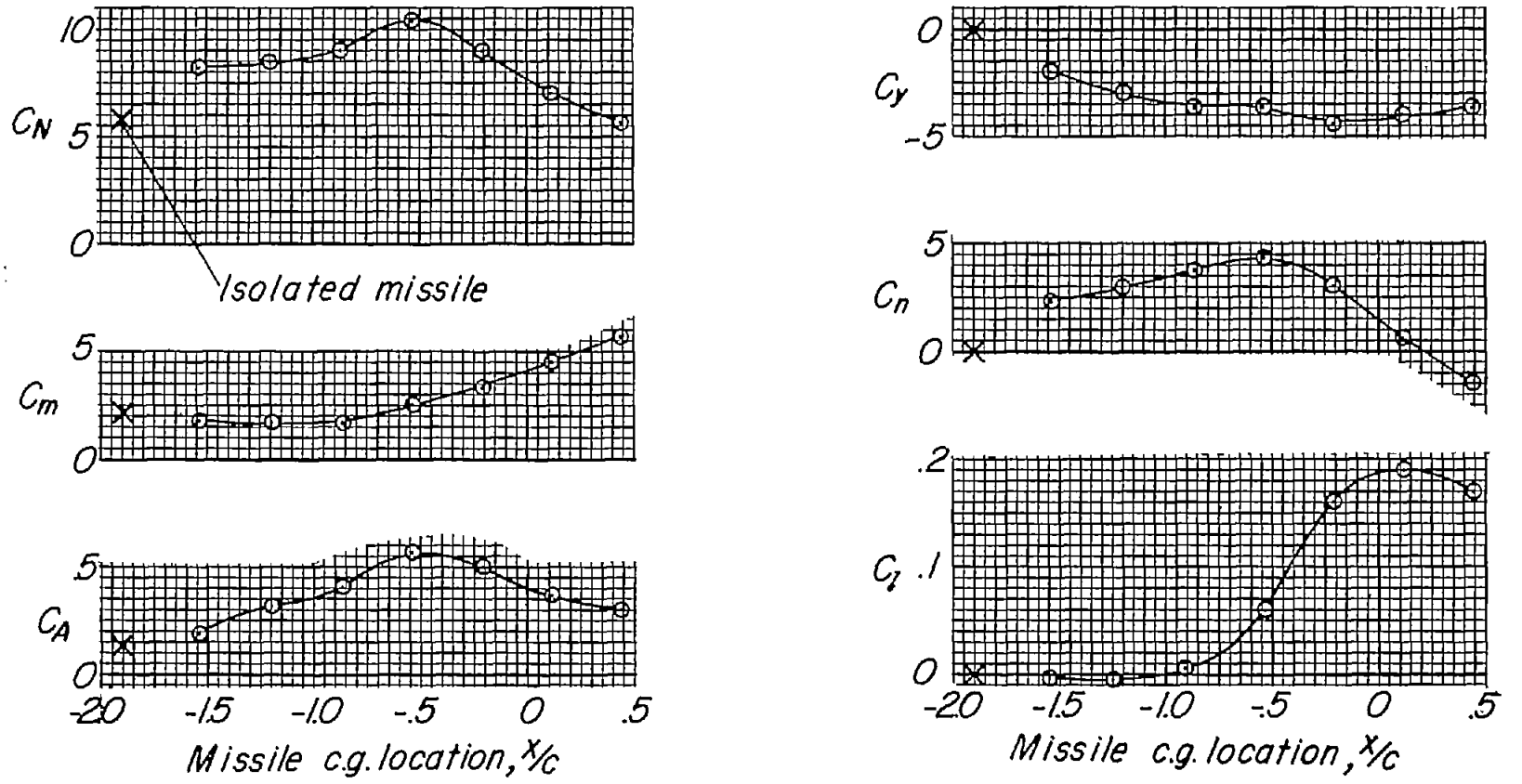

(g) $\alpha = 20^\circ$.

Figure 11.- Concluded.

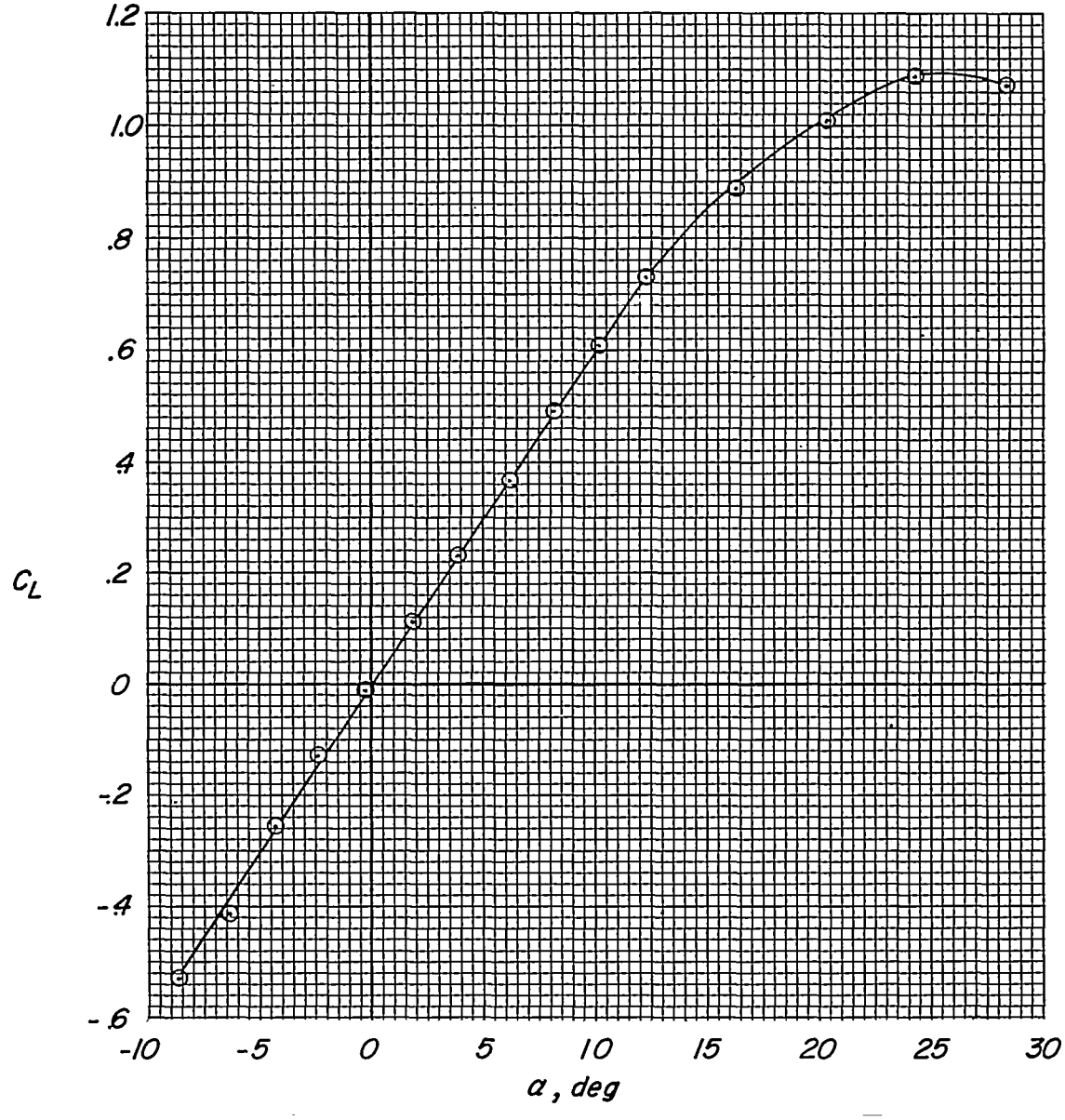

Figure 12.- Lift characteristics of isolated wing-fuselage combination.